PROHIBITIN3 Forms Complexes with ISOCHORISMATE SYNTHASE1 to Regulate Stress-Induced Salicylic Acid Biosynthesis in Arabidopsis[1][OPEN]

Aldo Seguel,[a] Joanna Jelenska,[b] Ariel Herrera-Vásquez,[a] Sharon K. Marr,[c] Michael B. Joyce,[b] Kelsey R. Gagesch,[b] Nadia Shakoor,[b] Shang-Chuan Jiang,[b] Alejandro Fonseca,[a] Mary C. Wildermuth,[c] Jean T. Greenberg,[b,2] and Loreto Holuigue[a,2]

[a]Departamento de Genética Molecular y Microbiología, Facultad de Ciencias Biológicas, Pontificia Universidad Católica de Chile, Santiago 8331150, Chile

[b]Department of Molecular Genetics and Cell Biology, University of Chicago, Chicago, Illinois 60637

[c]Department of Plant and Microbial Pathology, University of California, Berkeley, California 94720

ORCID IDs: 0000-0002-1575-1099 (A.S.); 0000-0001-6958-5949 (S.K.M.); 0000-0002-2035-7117 (N.S.); 0000-0001-7012-5739 (S.-C.J.); 0000-0002-1696-7385 (A.F.); 0000-0002-7213-7618 (J.T.G.); 0000-0001-7316-7504 (L.H.).

Salicylic acid (SA) is a major defense signal in plants. In Arabidopsis (*Arabidopsis thaliana*), the chloroplast-localized isochorismate pathway is the main source of SA biosynthesis during abiotic stress or pathogen infections. In the first step of the pathway, the enzyme ISOCHORISMATE SYNTHASE1 (ICS1) converts chorismate to isochorismate. An unknown enzyme subsequently converts isochorismate to SA. Here, we show that ICS1 protein levels increase during UV-C stress. To identify proteins that may play roles in SA production by regulating ICS1, we analyzed proteins that coimmunoprecipitated with ICS1 via mass spectrometry. The ICS1 complexes contained a large number of peptides from the PROHIBITIN (PHB) protein family, with PHB3 the most abundant. PHB proteins have diverse biological functions that include acting as scaffolds for protein complex formation and stabilization. PHB3 was reported previously to localize to mitochondria. Using fractionation, protease protection, and live imaging, we show that PHB3 also localizes to chloroplasts, where ICS1 resides. Notably, loss of PHB3 function led to decreased ICS1 protein levels in response to UV-C stress. However, *ICS1* transcript levels remain unchanged, indicating that ICS1 is regulated posttranscriptionally. The *phb3* mutant displayed reduced levels of SA, the SA-regulated protein PR1, and hypersensitive cell death in response to UV-C and avirulent strains of *Pseudomonas syringae* and, correspondingly, supported increased growth of *P. syringae*. The expression of a *PHB3* transgene in the *phb3* mutant complemented all of these phenotypes. We suggest a model in which the formation of PHB3-ICS1 complexes stabilizes ICS1 to promote SA production in response to stress.

The plant hormone salicylic acid (SA) plays diverse roles in development and stress defense responses (Vlot et al., 2009; Dempsey et al., 2011). Its developmental roles include the regulation of flowering time (Martínez et al., 2004), leaf longevity (slow cell death; Morris et al., 2000; Zhang et al., 2013), and biomass (Abreu and Munné-Bosch, 2009) in Arabidopsis (*Arabidopsis thaliana*) as well as thermogenesis in arum lily (*Sauromatum guttatum*) inflorescences (Raskin et al., 1987). Endogenous SA promotes seed germination under high-salinity conditions (Lee et al., 2010), basal thermotolerance (Clarke et al., 2004, 2009), and growth and development in the presence of the heavy metal cadmium (Guo et al., 2016). During biotic interactions with certain pathogens, SA is needed for the activation of plant defense responses that suppress pathogen growth (Vlot et al., 2009). Such responses can include the transcriptional up-regulation of a large number of pathogenesis-related (*PR*) genes (Uknes et al., 1992; Cao et al., 1997), rapid programmed cell death (the hypersensitive response; Coll et al., 2011; van Doorn et al., 2011), defense priming (Beckers et al., 2009;

[1] This work was supported by the National Commission for Science and Technology CONICYT (FONDECYT grant 1141202 to L.H.), the Millennium Science Initiative (Nucleus for Plant Synthetic and Systems Biology, grant NC130030 to Rodrigo Gutiérrez and L.H.), the National Institutes of Health (R01 GM54292 to J.T.G.), the National Science Foundation (NSF IOS-1456904 to J.T.G., NSF2010 0822393 to J.T.G. and Richard W. Michelmore, and NSF IOS-1449100 to M.C.W.). A.S. was supported by a PhD. fellowship from CONICYT, K.R.G was supported by NSF training grant 1062713, and N.S. by MCB training grant T32 GM 007183.

[2] Address correspondence to jgreenbe@uchicago.edu or lholuigue@bio.puc.cl.

The author responsible for distribution of materials integral to the findings presented in this article in accordance with the policy described in the Instructions for Authors (www.plantphysiol.org) is: Jean T. Greenberg (jgreenbe@uchicago.edu).

J.J., J.T.G., A.S., and L.H. designed the research; J.J., J.T.G., and L.H. supervised the experiments; A.S., J.J., A.H.-V., A.F., M.B.J., K.R.G., N.S., and S.-C.J. performed the experiments; A.S. and J.J. analyzed the data; S.K.M. and M.C.W. generated and tested the anti-ICS1 antibody; A.S., L.H., and J.T.G. wrote the article with contributions from the other authors.

[OPEN] Articles can be viewed without a subscription.

www.plantphysiol.org/cgi/doi/10.1104/pp.17.00941

Tateda et al., 2014; Zhang et al., 2014), and systemic immunity to new infections (Fu and Dong, 2013).

A major mechanism of SA deployment is through its increased synthesis in response to pathogens and abiotic stresses, such as treatments with UV-C light, high-light radiation, and ozone (Yalpani et al., 1994; Nawrath et al., 2002; Ogawa et al., 2005; Mateo et al., 2006; Catinot et al., 2008; Garcion et al., 2008). Interestingly, the Enhanced Disease Susceptibility5 (EDS5) SA transporter in the chloroplast envelope of Arabidopsis is necessary for stress-induced SA accumulation, possibly due to a regulatory coupling of SA transport and synthesis (Serrano et al., 2013; Yamasaki et al., 2013). Recently, a catabolic enzyme that converts SA to 2,3-dihydroxybenzoic acid in Arabidopsis was described (Zhang et al., 2013). Other enzymes that impact SA levels have been found or inferred from the presence of metabolites related to SA (Mauch et al., 2001; Nugroho et al., 2001; Vlot et al., 2009; Simoh et al., 2010; Dempsey et al., 2011; Zhang et al., 2017).

In plants, there is evidence for two biosynthetic routes for SA: the isochorismate (IC) and the Phenylalanine ammonia lyase (PAL) pathways. As a precursor, both pathways use chorismate, which is the end product of the shikimate pathway that operates in plastids (Poulsen and Verpoorte, 1991; Schmid and Amrhein, 1995). The IC pathway has two steps. One is the reversible conversion of chorismate to IC catalyzed by ISOCHORISMATE SYNTHASE1 (ICS1), a plastid-localized enzyme (Strawn et al., 2007). The second step is the conversion of IC to SA by a mechanism that is still unknown in plants (Strawn et al., 2007).

The regulation of SA production under stress conditions through ICS activity differs in different plant species. In Arabidopsis, most of the basal SA is produced via the PAL pathway (Huang et al., 2010), whereas the IC pathway is responsible for approximately 90% of SA production induced by pathogens or UV-C light (Wildermuth et al., 2001; Garcion et al., 2008). However, it has been shown that, unlike Arabidopsis, the PAL and IC pathways are equally important for pathogen-induced SA biosynthesis in soybean (*Glycine max*; Shine et al., 2016). Both Arabidopsis and soybean have two *ICS* genes. In other land plants, such as poplar (*Populus trichocarpa*), rice (*Oryza sativa*), castor bean (*Ricinus communis*), grapevine (*Vitis vinifera*), and alfalfa (*Medicago truncatula*), alternative splicing of a single *ICS* gene works as a mechanism to modulate ICS function (Macaulay et al., 2017). Therefore, differential ICS regulation may have evolved to accommodate the chemical defense strategies of different plants (Yuan et al., 2009).

The level of SA in different tissues after stress treatment was suggested to be critical for defining the type of defense reaction that is established (Fu et al., 2012). Therefore, knowledge of how SA levels are controlled is a central issue for understanding plant defense responses and stress physiology. A number of proteins are needed for normal SA accumulation due to their regulatory and signaling roles in defense (Lu et al., 2003; Song et al., 2004; Okrent et al., 2009; Nomura et al., 2012; Wang et al., 2014; Ding et al., 2015; Cui et al., 2017). Transcriptional regulators of the *ICS1* gene also have been studied (Chen et al., 2009; Zhang et al., 2010; Dempsey et al., 2011; van Verk et al., 2011; Zheng et al., 2012, 2015; Wang et al., 2015). However, proteins implicated in the direct regulation of ICS1 protein and/or activity levels have yet to be documented. In this study, proteins found to coimmunoprecipitate with ICS1 were identified, and the role of one of them, PROHIBITIN3 (PHB3), is characterized. PHBs play important and diverse biological functions, such as acting as scaffold proteins for complex formation and stabilization (Steglich et al., 1999; Nijtmans et al., 2000; Van Aken et al., 2007). Many molecular studies in diverse organisms, such as yeast, mammals, and plants, have focused on the roles of PHBs in mitochondria (Steglich et al., 1999; Nijtmans et al., 2000; Piechota et al., 2010). The current view is that the principal function of PHBs in mitochondria is to support the structural organization of the inner mitochondrial membrane (Piechota et al., 2015). In plants, PHBs play a positive role in the development of new tissues and organs, possibly by maintaining optimal mitochondrial activity (Ahn et al., 2006; Van Aken et al., 2007). We show here that PHB3 impacts both ICS1 protein and SA accumulation and is found in chloroplasts, making it a potentially direct regulator of this important pathway.

RESULTS

Identification of PHBs as Proteins That Form Complexes with ICS1

We took advantage of previously constructed *sid2-2* plants that contain a complementing *ICS1-V5* transgene (Strawn et al., 2007) to identify proteins with which ICS1 forms complexes using affinity purification and proteomics. V5 antibody-conjugated beads were used to immunoprecipitate proteins from extracts of untreated and UV-C-treated *sid2-2/ICS1-V5* or wild-type plants. Liquid chromatography-tandem mass spectrometry (LC-MS/MS) analysis showed that, together with ICS1 peptides, a large number of peptides from a family of proteins called PHBs (Table I; Supplemental Table S1) were found in immunoprecipitates from the ICS1-V5 plant extracts. Supplemental Figure S1 shows the enrichment of PHBs using spectral counting, and Supplemental Table S1 shows the top proteins from which peptides were found to be specifically enriched, including PHB3, PHB2, PHB4, and several proteins in the superfamily to which PHBs belong (called Band 7). Immunoblotting using an antibody that recognizes PHB3 and PHB4 (Snedden and Fromm, 1997; Van Aken et al., 2007) confirmed that PHB3/4 proteins were present in the ICS1-containing complexes (Fig. 1A). It was shown previously that the majority of the immunoblot signal found with this antibody comes from PHB3 (Van Aken et al., 2007). The amount of ICS1 and PHB3/4 recovered after immunoprecipitation of

Table I. *PHBs found in ICS1-V5 complexes purified from sid2-2/ICS1-V5 plants*

Peptides were identified by LC-MS/MS analysis. Unique Peptides indicates the number of different peptides that match the indicated protein and also may match one or more other isoforms. Specific Peptides indicates the number of peptides specific to the protein isoform indicated. Percentage Coverage shows the percentage of the protein sequence represented by the peptides found in the LC-MS/MS analysis. AGI, Arabidopsis Genome Initiative.

Proteins	AGI Number	Unique Peptides	Specific Peptides	Percentage Coverage
ICS1	AT1G74710	16	13	42
PHB3	AT5G40770	19	11	69
PHB2	AT1G03860	16	9	64
PHB4	AT3G27280	12	4	53
PHB6	AT2G20530	9	4	37
PHB1	AT4G28510	8	4	39

ICS1-V5 was unaffected by UV-C light 24 h post treatment (Fig. 1, B and C). These results indicate that the ICS1 protein forms complexes with PHBs.

ICS1 Protein Levels Are UV-C Inducible

ICS1 transcript and SA levels are induced by UV-C stress in Arabidopsis (Shapiro and Zhang, 2001; Nawrath et al., 2002; Martínez et al., 2004; Garcion et al., 2008; Serrano et al., 2013). As expected, under our conditions, UV-C induced *ICS1* transcript levels in wild-type plants (Fig. 2A, left). Immunoblot analysis using an antibody that specifically recognizes ICS1 showed that UV-C also induced ICS1 protein accumulation in the wild type but not in the negative control (*sid2-2* mutant plants; Fig. 2B).

These results contrasted with what was observed in *sid2-2/ICS1-V5* plants. In particular, *sid2-2/ICS1-V5* plants had high levels of both ICS1-V5 transcript and protein even without stress (Fig. 2, A, C, and D; see also Fig. 1). ICS1 protein levels were so high in the ICS1-V5 plants that the immunoblots were completely overexposed under conditions where ICS1 protein could be detected with the ICS1 antibody in the wild type (Fig. 2C). Therefore, the blot in Figure 2C was stripped and reprobed with V5 antibody. In *sid2-2/ICS1-V5* plants, basal levels of PR1 and SA were elevated (Fig. 2, D and E). Although significant differences in ICS1-V5 transcript or protein levels in response to UV-C were not detected at the time points tested (Fig. 2, A and D), SA and PR1 were elevated (Fig. 2, D and F). Basal levels of SA in *sid2-2/ICS1-V5* were affected by the growth conditions: soil-grown plants (Fig. 2E) showed higher levels of SA than in vitro-grown plants (Fig. 2F). These results indicate that the ICS1 protein accumulates upon UV-C stress exposure in wild-type plants.

PHB3 Localizes to Chloroplasts and Mitochondria

Since ICS1 forms complexes with PHB3/4 and other PHBs, a pool of PHBs may be present in chloroplasts where ICS1 localizes (Strawn et al., 2007). Previously, PHB3 was described as a mitochondrial protein (Ahn et al., 2006; Van Aken et al., 2007). To evaluate the subcellular localization of PHB3, we used confocal microscopy for live imaging of PHB3-GFP and organelle markers transiently expressed in *Nicotiana benthamiana*, and PHB3-GFP constitutively expressed in Arabidopsis. The PHB3-GFP fusion was functional, as it could rescue the known small-plant phenotype of an Arabidopsis *phb3-3* loss-of-function mutant (Wang et al., 2010; Fig. 3A). This mutant was confirmed to have reduced levels of PHB3 (Supplemental Fig. S2). The control, untransformed *N. benthamiana* leaves showed very little background signal under our imaging conditions (Fig. 3B; Supplemental Fig. S3). PHB3-GFP localized in chloroplasts and small structures resembling mitochondria in both species (Fig. 3, C–E). A portion of the PHB3-GFP signal colocalized with chlorophyll autofluorescence (Fig. 3C; Supplemental Fig. S3; Supplemental Video S1). Additionally, PHB3-GFP colocalized with OEP7-RFP, a marker for the envelope membrane of chloroplasts, around *N. benthamiana* chloroplasts (Lee et al., 2011; Fig. 3C; Supplemental Fig. S3). Stable Arabidopsis transformants also showed colocalization of a portion of the PHB3-GFP signal with chlorophyll autofluorescence in epidermal chloroplasts (Fig. 3D; Supplemental Fig. S3).

A portion of the PHB3-GFP signal outside chloroplasts colocalized in small structures with the mitochondrial markers COX4-mCherry (Nelson et al., 2007) and COX4-dsRed (Li et al., 2017) in *N. benthamiana* (Fig. 3E; Supplemental Fig. S3). PHB3-GFP also was visible in similar structures in Arabidopsis (Fig. 3D). Videos of transiently transformed *N. benthamiana* show characteristic mobility of the mitochondria labeled with PHB3-GFP and COX4-mCherry (Supplemental Videos S1 and S2).

To confirm the chloroplast localization of PHB3 and cofractionation with ICS1, we isolated chloroplasts from *sid2-2/ICS1-V5* plants treated or not with UV-C and performed immunoblot analysis. Chloroplasts from untreated wild-type plants also were assessed for PHB3/4 localization. PHB3/4 was detected in chloroplast fractions of untreated wild-type plants as well as in untreated and UV-C-treated *sid2-2/ICS1-V5* plants (Fig. 4A). As expected, ICS1-V5 was detected in the chloroplasts of untreated and treated *sid2-2/ICS1-V5*

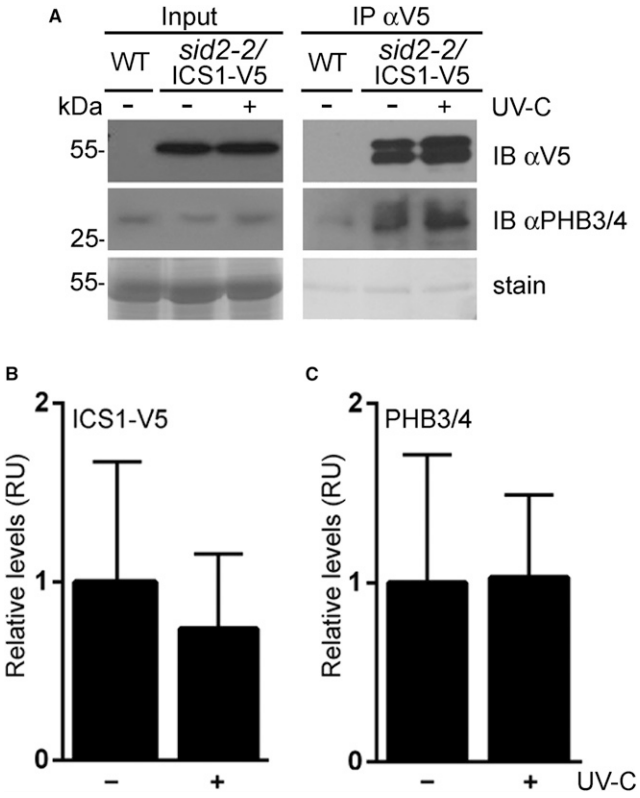

Figure 1. PHB3/4 form complexes with ICS1-V5 under normal and stress conditions. A, Plants grown in soil were treated with UV-C light for 45 min and assayed 24 h later (+). Untreated plants were used as controls (−). Total proteins were extracted, and ICS1-containing complexes were immunoprecipitated with V5 antibody. The presence of ICS1-V5 and PHB3/4 proteins in the total protein extracts (Input; left) and in the immunoprecipitated ICS1-containing complexes (IP αV5; right) was confirmed by immunoblotting (IB) using V5 and PHB3/4 antibodies. Coomassie Blue-stained membranes (bottom) show similar loading. Representative blots from three independent experiments (two from total extracts and one from chloroplast extracts) are shown. WT, Wild type. B and C, Quantitation of ICS1-V5 (B) and PHB3/4 (C) protein levels from three immunoprecipitation experiments as in A, using densitometry with the ImageJ program. RU, Relative units with respect to an average signal of untreated samples for each antibody. Error bars show SE. Statistical analyses using Student's *t* tests showed that no significant differences were detected ($P = 0.78$ for B and $P = 0.97$ for C).

plants. We did not observe changes of PHB3/4 or ICS1 localization upon UV treatment. The immunodetection of protein markers for different subcellular fractions confirmed the purity of the chloroplast fractions. Importantly, chloroplasts were not contaminated with the mitochondrial marker peroxiredoxin II F (Prx IIF; Fig. 4A).

PHB is associated with membranes in mitochondria (Tatsuta et al., 2005; Piechota et al., 2010). To test the localization of PHB in chloroplasts, we partitioned isolated chloroplasts into membrane and soluble fractions (Fig. 4B). PHB was detected with the PHB3/4 antibody in the membrane but not in the soluble fractions of Arabidopsis, spinach (*Spinacia oleracea*), and *N. benthamiana* chloroplasts. The purity of the fractions was confirmed by immunodetection of inner envelope Tic110 and stromal cpHsp70 proteins (Fig. 4B).

To test if PHB is a peripheral or internal chloroplast protein, we treated isolated *N. benthamiana* and Arabidopsis chloroplasts with thermolysin to remove surface proteins (Fig. 4, C and D). Transiently produced AtPHB3-GFP in *N. benthamiana* as well as the native PHBs in *N. benthamiana* (Fig. 4C) and Arabidopsis (Fig. 4D) chloroplasts were mostly protected from thermolysin. We observed partial proteolysis of the chloroplast inner envelope protein Tic110 (Jackson et al., 1998; Inaba et al., 2003) in both species (Fig. 4, C and D), as reported previously (Hardré et al., 2014). The outer envelope protein SFR2 from Arabidopsis, detected with an antibody that did not recognize the *N. benthamiana* protein (Roston et al., 2014), was digested by thermolysin (Fig. 4D). In contrast, the thylakoid membrane-associated proteins ATP synthase β (AtpB) and light-harvesting complex II (LHCII), as well as the stromal cpHSP70, were fully protected from proteolysis (Fig. 4, C and D). Together, these data demonstrate that a pool of PHB3 localizes to chloroplasts, most likely to the inner envelope. This result is consistent with the finding that this protein forms complexes with ICS1.

SA and PR1 Levels in Response to UV-C Treatment and Bacterial Infections Are Reduced in the *phb3-3* Mutant

Since ICS1 forms complexes with PHB3, we evaluated whether the *phb3-3* mutant is compromised for SA biosynthesis and/or SA-dependent responses after UV-C stress. After UV-C treatment for 24 h, *phb3-3* mutant plants showed reduced SA levels compared with the wild type. However, SA levels in *phb3-3* were not as low as those in the SA biosynthesis mutant *sid2-2* (Fig. 5A). The SA response marker PR1 also showed lower levels in *phb3-3* than in the wild type (Fig. 5B). UV-C failed to induce PR1 in *sid2-2* (Fig. 5C), confirming that this marker is SA dependent under these conditions. Importantly, PR1 was induced in the *phb3-3* mutant upon SA treatment, indicating that this mutant still responds to SA (Fig. 5D).

We also evaluated whether the *phb3-3* mutant was compromised for SA accumulation and responses after infection with a pathogen that induces SA. For this purpose, wild-type and *phb3-3* plants were inoculated by flooding (Ishiga et al., 2011) with an avirulent strain of *Pseudomonas syringae* pv *tomato* DC3000 carrying AvrRpm1 (*Pst/AvrRpm1*). Compared with the wild type, *phb3-3* plants showed lower free SA levels 12 h after infection (Fig. 6A), a phenotype that we found previously to strongly correlate with hypersusceptibility (Lu et al., 2003; Song et al., 2004; Lee et al., 2007). Additionally, glycosylated SA levels were lower in *phb3-3* mutant plants compared with the wild type throughout the time course (Fig. 6A). We also detected a lower accumulation of PR1 protein in *phb3-3* mutant

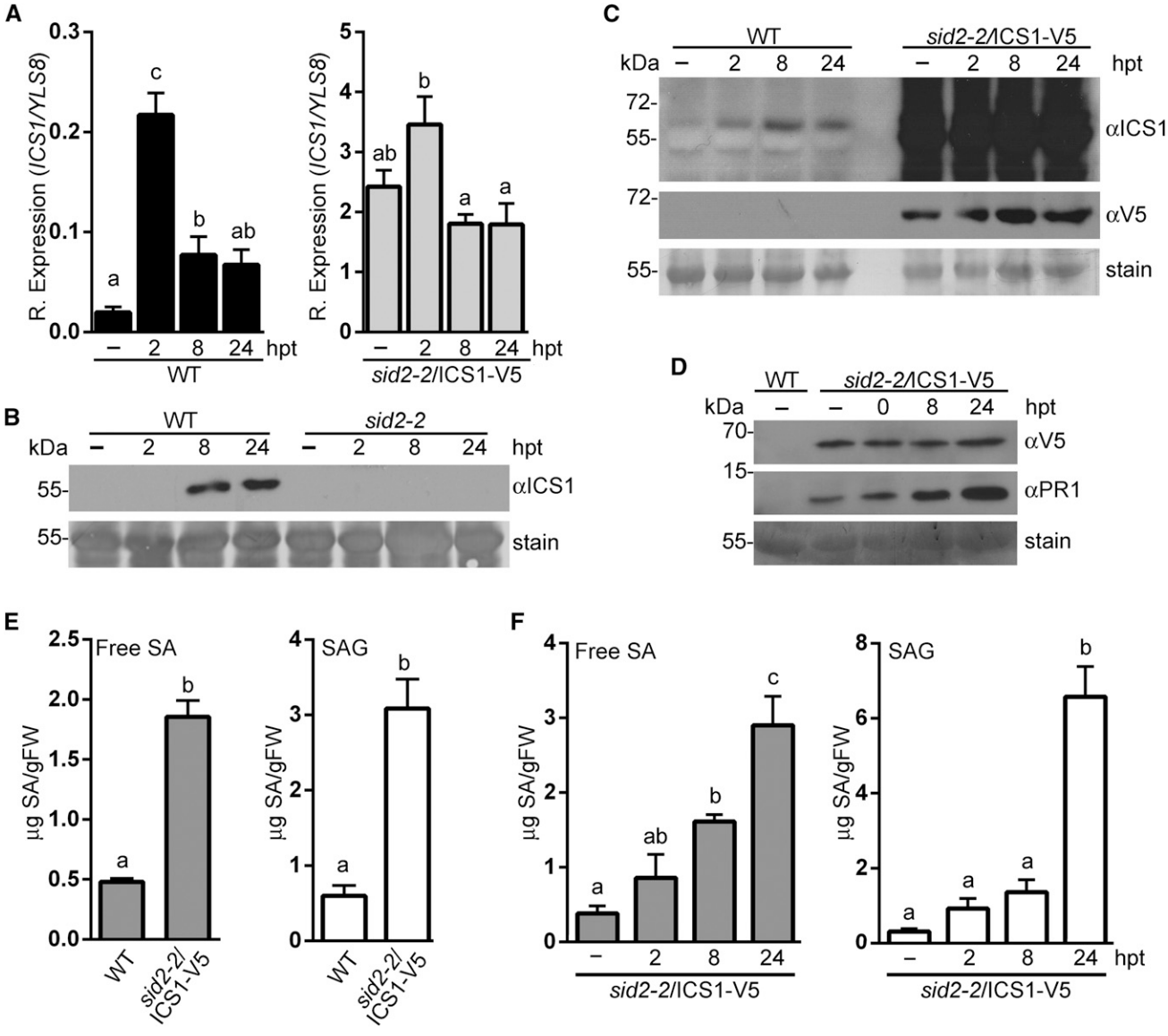

Figure 2. ICS1 protein levels are induced by UV-C treatment and constitutively elevated in *sid2-2/ICS1-V5* plants. Plants grown on plates (A, B, C, and F) or soil (D) were treated with UV-C for 20 min (A, B, C, and F) or 45 min (D), and assayed 0, 8, and 24 h post treatment (hpt). Untreated plants were used as controls (–). A, *ICS1* transcript levels were measured by RT-qPCR in wild-type (WT; black bars) and *sid2-2/ICS1-V5* (gray bars) plants. Expression is relative (R.) to the *YLS8* gene ($n = 3$ biological replicates). B, Immunoblot analysis showing that ICS1 is induced by UV-C treatment in the wild type and is not detectable in *sid2-2* plants. C, ICS1 protein levels detected by immunoblot in wild-type and *sid2-2/ICS1-V5* plants using ICS1 or V5 antibodies. D, PR1 and ICS1-V5 protein levels in wild-type and *sid2-2/ICS1-V5* plants. In *sid2-2/ICS1-V5* plants, basal PR1 is elevated and UV-C further induces the PR1 level. In B to D, representative results from three (B and C) or two (D) independent experiments are shown. Coomassie Blue-stained membranes (bottom) show similar loading. E and F, Free SA (gray bars) and glycosylated SA (SAG; white bars) levels in the indicated plants. E, Untreated plants grown in soil, showing higher SA levels in *sid2-2/ICS1-V5* plants than in the wild type ($n = 5$). Similar results were found in an independent trial. F, Free SA and SAG levels are induced by UV-C in plants with constitutive ICS1 levels ($n = 3$). FW, Fresh weight. Statistical analyses in A and F were performed using ANOVA/Fisher's LSD test and in E using Student's *t* test. Each letter group differs from other letter groups at $P < 0.05$. Error bars show SE.

plants compared with wild-type plants after infection (Fig. 6B).

As predicted by the reduced SA accumulation, *phb3-3* mutant plants showed greater growth of *Pst/AvrRpm1* compared with the wild type, similar to the *sid2-2* mutant phenotype (Fig. 7A). The *phb3-3* mutant also was more susceptible to the avirulent strain *Pst/AvrRpt2* and showed similar levels of bacterial growth to *sid2-2* (Fig. 7B). This result was expected, since *Pst/AvrRpt2* normally triggers SA-dependent disease

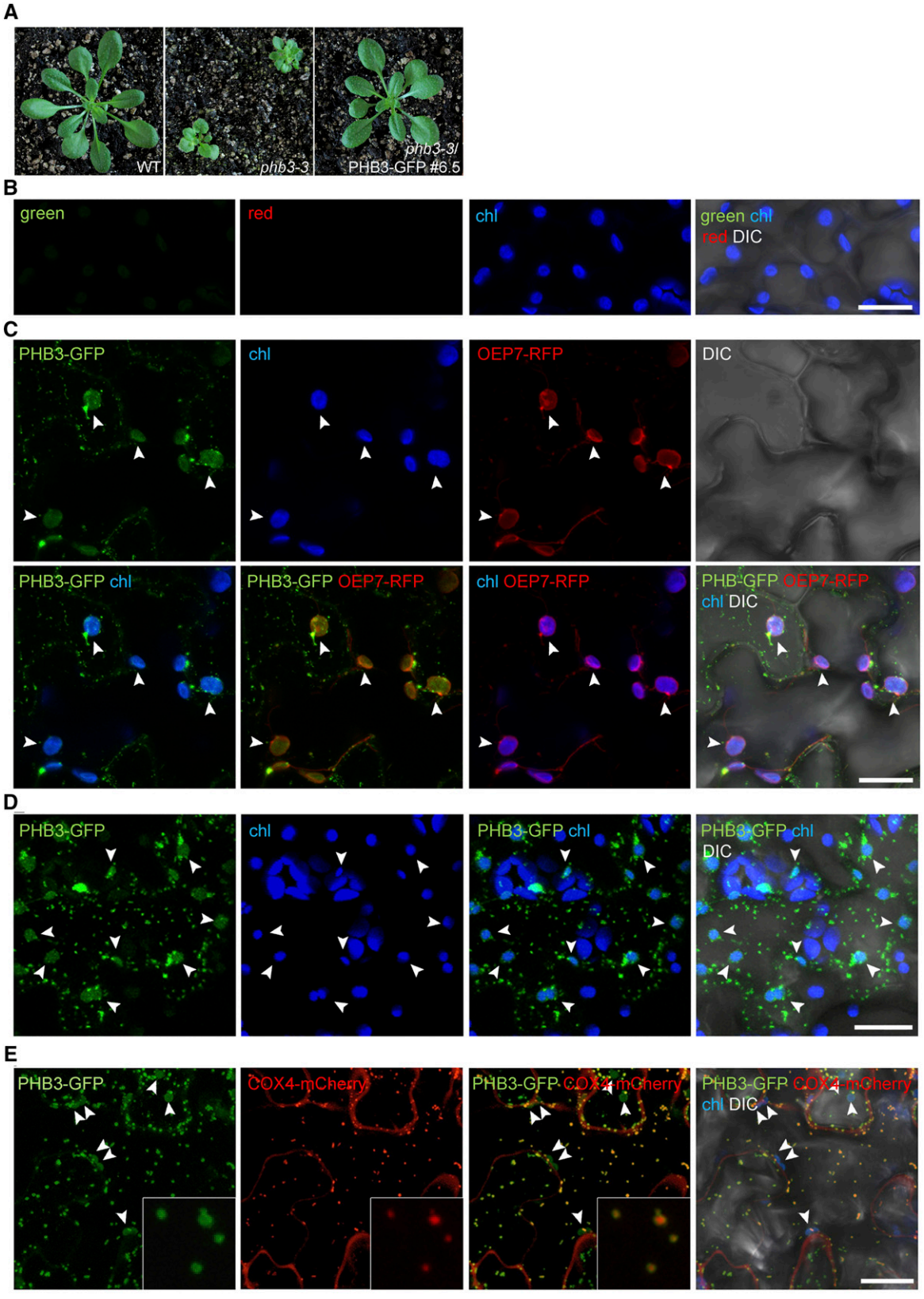

Figure 3. PHB3-GFP localizes to chloroplasts and mitochondria. A, The morphological phenotype of the *phb3-3* mutant is complemented by the *PHB3-GFP* transgene. Images show 3-week-old wild-type (WT), *phb3-3*, and *phb3-3/PHB3-GFP* #6.5 plants grown in soil. B to E, Untransformed (B) and transiently transformed (C and E) *N. benthamiana* leaves, and stably

resistance (Nawrath and Métraux, 1999). In wild-type plants, these two pathogen isolates induce hypersensitive cell death that can be detected at the individual cell level (Kim et al., 2005). To monitor this, we performed light microscopy of leaves stained with Trypan Blue within 10 h of infection. Both *phb3-3* and *sid2-2* showed reduced Trypan Blue staining relative to the wild type after inoculation with *Pst/AvrRpm1* and *Pst/AvrRpt2* strains (Fig. 7, C and D). Similar phenotypic effects of *sid2* mutations on single cell death events were reported previously (Brodersen et al., 2005; Ichimura et al., 2006; Yao and Greenberg, 2006; Lu, 2009).

These experiments show that PHB3 promotes SA production during stress and infection and is needed for SA-dependent processes such as the suppression of pathogen growth and the hypersensitive response at the single cell level.

Expression of PHB3 Complements *phb3-3* Mutant Plants in Abiotic and Biotic Stress Responses

To determine whether the main phenotypes observed in *phb3-3* mutant plants were due to the lack of PHB3 function, we transformed the mutant with a *pUBQ10*:*PHB3-V5* rescue construct. The small-plant phenotype of *phb3-3* was complemented in transgenic lines *PHB3-V5* #15 and *PHB3-V5* #17 (Fig. 8A). The production of PHB3-V5 protein in both lines was verified by immunodetection of the V5 epitope (Fig. 8B). We noticed that, in *phb3-3* leaf cross sections, the tissue morphology appeared less organized than in the wild type, a phenotype that also was complemented by the PHB3 transgene (Fig. 8C). Importantly, the complemented lines were restored for the UV-C-induced SA and PR1 as well as the pathogen resistance phenotypes (Fig. 8, D–F). These results confirm that the phenotypes we observed are due to the *phb3-3* mutation.

PHB3 Regulates ICS1 Protein Levels

Since SA levels were decreased in UV-C-stressed *phb3-3* plants, we evaluated the effect of the *phb3-3* mutation on ICS1 levels. *ICS1* transcript levels in wild-type, *phb3-3*, and *phb3*-3/*PHB3-V5* complemented plants treated with UV-C light increased similarly, with a peak at 2 h after irradiation (Fig. 9A). These data suggest that the regulation of ICS1 by PHB3 may occur at the posttranscriptional level. A decrease in the ICS1 protein levels was detected in *phb3-3* plants after the UV-C treatment compared with the wild type (Fig. 9B). Furthermore, we detected an increase in ICS1 protein levels in the PHB3-V5 complemented lines (Fig. 9B) relative to wild-type levels, in agreement with the increase in SA levels detected in these lines (Fig. 8D).

In contrast to ICS1, the levels of the chloroplast proteins Tic110, NOA1, AtpB, and lipooxygenase2 (LOX2) were not altered significantly in the *phb3-3* mutant compared with the wild type (Fig. 9C). Although *phb3-3* affects stressed-induced nitric oxide accumulation in roots (Wang et al., 2010), we did not observe differences in the levels of NOA1, a chloroplast protein involved in nitric oxide regulation (Mandal et al., 2012), between *phb3-3* and wild-type leaves (Fig. 9C). These data indicate that *phb3-3* does not have a general effect on chloroplast proteins.

These results strongly suggest that PHB3 regulates SA accumulation through the formation of complexes and stabilization of the ICS1 protein under stress conditions.

DISCUSSION

Several lines of evidence from this work suggest that increased SA production during UV-C stress involves the induction of active ICS1-containing multiprotein complexes. First, in wild-type Arabidopsis, ICS1 protein levels increase upon UV-C stress. Second, ICS1 forms complexes with PHB3/4 and other PHBs. Third, during stress, ICS1 protein (but not RNA) levels and the downstream accumulation of SA show alterations that are correlated with the amount of functional PHB3 in plants. Our findings support the view that PHB3-ICS1 complexes are needed for the full production of SA during stress caused by UV-C.

The role of PHB3 in promoting SA production extends beyond the response to UV-C stress to the biotic interaction of Arabidopsis with the strongly SA-inducing (avirulent) bacterial strain *Pst/AvrRpm1*. The *phb3-3* mutant is hypersusceptible to this strain as well as to the avirulent strain *Pst/AvrRpt2*. Thus, it is possible that PHB3 is necessary to promote maximal SA production when the need for this defense signal is high, such as during stress and other biotic interactions.

It is interesting that, even though there is residual SA accumulation in the *phb3-3* plants after infection, the mutant is as susceptible to two avirulent *Pst* strains and

Figure 3. (*Continued.*)
transformed Arabidopsis cotyledons (D), were imaged by confocal microscopy in green (PHB3-GFP), red (OEP7-RFP and COX4-mCherry), chlorophyll autofluorescence (chl; blue), and differential interference contrast (DIC; bright-field) channels. Maximum intensity projections of Z series images are shown. C, Coexpression of PHB3-GFP and OEP7-RFP (chloroplast outer envelope marker). D, Expression of PHB3-GFP in Arabidopsis (*phb3-3/PHB3-GFP* #6.5 plants). E, Coexpression of PHB3-GFP and COX4-mCherry (mitochondrial marker). Insets show higher magnification. Colocalization with COX4-dsRed also was performed with similar results. White arrowheads show examples of PHB3-GFP localization in chloroplasts (C–E). Experiments were done two (D) or three (B, C, and E) times with similar results. Bars = 20 μm.

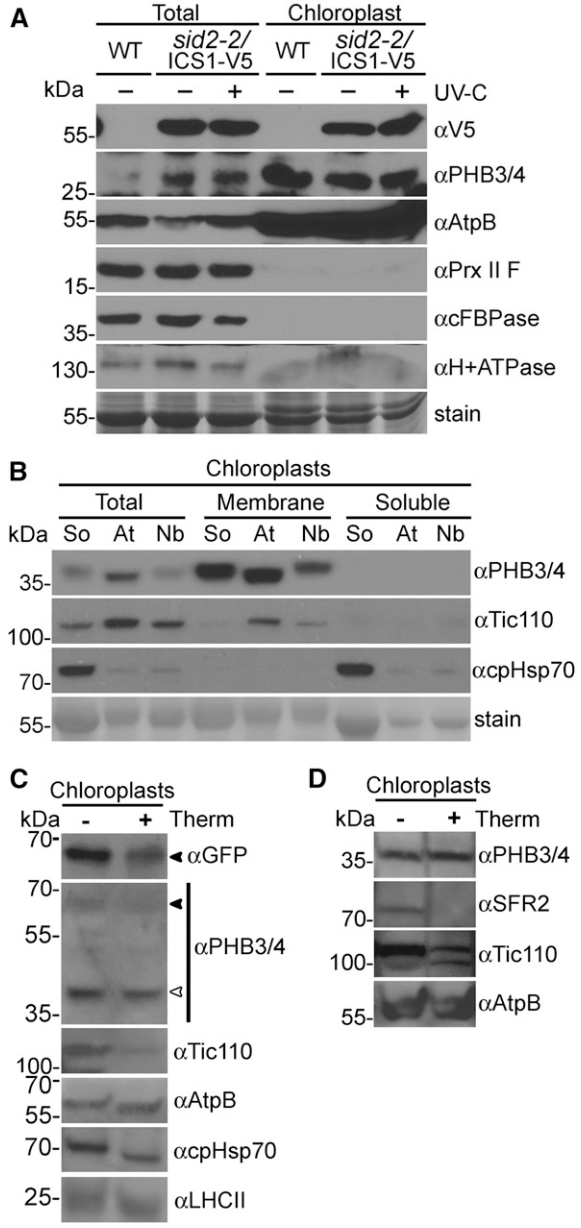

Figure 4. PHB3 is a chloroplast membrane protein. A, Immunodetection of PHB3/4 in total and chloroplast protein extracts obtained from wild-type (WT) and *sid2/ICS1-V5* plants, grown in soil, treated (+) or not (–) with UV-C as described in Figure 1. ICS1-V5 was detected with V5 antibody, and PHBs were detected with a PHB3/4 antibody ($n = 2$). The purity of the chloroplast fraction was evaluated by immunodetection of markers for specific subcellular localizations (AtpB for chloroplast, Prx II F for mitochondria, cytosolic Fru-1,6-bisphosphatase [cFBPase] for cytoplasm, and H^+-ATPase for plasma membrane). B, PHB3 localizes to chloroplast membranes. Spinach (So), Arabidopsis (At), and *N. benthamiana* (Nb) chloroplasts were partitioned into membrane and soluble fractions. PHB was detected with a PHB3/4 antibody, and fractions were confirmed with antibodies against pea Tic110 (membrane) and spinach cpHsp70 (soluble). Coomassie Blue (A) and Ponceau S (B) staining of proteins show similar loading. C and D, PHB is mostly protected from thermolysin digestion in *N. benthamiana* (C) and Arabidopsis (D) chloroplasts. Chloroplasts isolated from *N. benthamiana* transiently expressing AtPHB3-GFP (C; top four gels), control *N. benthamiana* (C; bottom two gels), or Arabidopsis leaves (D) were incubated without (−) or with (+) thermolysin (Therm). Sensitivity to digestion was evaluated for PHB (PHB3/4 antibody), AtPHB3-GFP (GFP antibody and PHB3/4 antibody; C), the inner envelope Tic110, the outer envelope SFR2 (D), the thylakoid-associated AtpB, and LHCII and the stromal cpHsp70 (C). Black arrowheads indicate AtPHB3-GFP, and the white arrowhead shows NbPHB (C). Similar results were obtained for two to four chloroplast preparations.

shows similar hypersensitive cell death suppression as *sid2-2* (an SA biosynthesis mutant). One possible explanation for the strong phenotypes of *phb3-3* plants is that this mutant fails to sense SA adequately; therefore, a normal defense response is not activated. However, the *phb3-3* plants respond normally to exogenous SA treatment, indicating that SA signaling is not altered. Instead, the strong phenotype of *phb3-3* might be the result of a delay in these plants to fully induce SA. We speculate that there is a threshold level of SA that is needed early after infection to promote the induction of defenses that suppress the growth of *P. syringae*. Alternatively, SA-independent signal(s) that are affected in the *phb3-3* plants under some conditions, such as nitric oxide (Wang et al., 2010) or ethylene (Christians and Larsen, 2007), also may contribute to plant defense. However, other Arabidopsis plants with reduced SA production, generated by altered expression/mutation of genes that impact SA biosynthesis, exhibit enhanced susceptibility to virulent and avirulent pathogens, similar to the phenotype of *phb3-3* (Delaney et al., 1994; Nawrath and Métraux, 1999; Dewdney et al., 2000; Lu et al., 2003; Song et al., 2004; Lee et al., 2007).

In addition to identifying the localization of PHB3 in mitochondria (Van Aken et al., 2007; Piechota et al., 2010), this work established that there is a pool of PHB3 that resides in chloroplasts, the organelle where SA is made and where ICS1 is targeted (Strawn et al., 2007; Fragnière et al., 2011). PHB3 has a hydrophobic region at the N terminus that likely serves to anchor it to membranes. In agreement with this, PHB3 fractionated with chloroplast membranes and was mostly protected from thermolysin proteolysis, while PHB3-GFP fluorescence was detected at the periphery of chloroplasts, similar to an envelope marker. This study thus establishes that PHB3 is targeted to chloroplasts, similar to PHB2 and PHB4, which were reported previously to be in the envelope fraction of chloroplasts in a proteomics study (Kleffmann et al., 2004).

PHB3 was found previously to copurify with PHB1, PHB2, PHB4, and PHB6 (Van Aken et al., 2007). It was also described as residing in two very large (1–2 MD) mitochondrial inner membrane complexes with this same group of PHBs (Piechota et al., 2010). These five PHBs all coimmunoprecipitate with ICS1. The mitochondrial matrix AAA protease FTSH10 immunoprecipitates four of the five PHBs (except PHB4) that we identified in ICS1 complexes as well as FTSH3 (Piechota et al., 2010). This result suggests that at least four PHBs

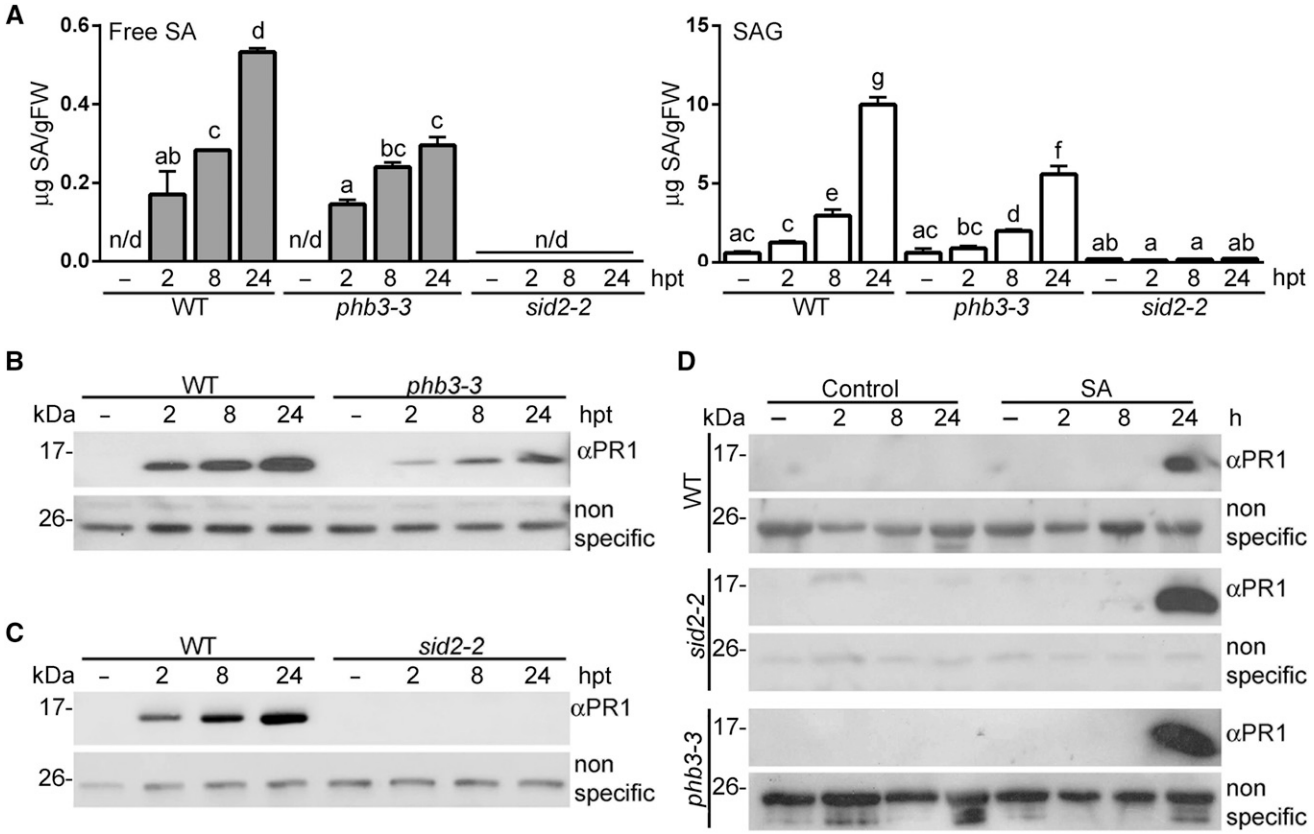

Figure 5. *phb3-3* mutant plants have lower SA levels and PR1 accumulation after UV-C treatment. A to C, Leaf tissue from plants grown on plates treated with UV-C light for 20 min and harvested at 2, 8, and 24 h post treatment (hpt). Untreated plants were used as controls (–). A, Levels of free SA (gray bars) and glycosylated SA (SAG; white bars). FW, Fresh weight; n/d, not detected. Each bar represents the mean of three independent experiments; error bars indicate SE. Statistical analysis was performed using ANOVA/Fisher's test. Different letters denote statistically significant differences at $P < 0.05$. B and C, PR1 protein was detected by immunoblot analysis using a PR1 antibody. A nonspecific band in the immunoblot shows similar loading in each lane. Gels show representative results from three independent experiments. D, Two-week-old wild-type (WT), *phb3-3*, and *sid2-2* plants grown on plates were treated with liquid Murashige and Skoog (MS) growth medium alone (Control) or MS medium supplemented with 0.5 mM SA for 2, 8, and 24 h. – indicates untreated plants. PR1 protein was detected by immunoblot analysis as in B and C. An independent trial of this experiment showed similar results.

may form complexes together in more than one subcellular compartment along with one or more non-PHB proteins (FTSH10 and FTSH3 in mitochondria and ICS1 in chloroplasts). PHBs form ring-like structures in the inner mitochondrial membrane (Tatsuta et al., 2005; Piechota et al., 2010). If PHBs are capable of forming similar structures/complexes in the chloroplast envelope, they may facilitate the import of ICS1 to this organelle or affect its stability after import. Future work will focus on whether PHBs act as chaperones and whether they form large complexes within chloroplasts.

How might PHBs regulate ICS1 levels and/or activity? Using an assay in which radiolabeled ICS1 was imported into isolated pea (*Pisum sativum*) chloroplasts and then fractionated, Strawn et al. (2007) showed that the majority of ICS1 partitioned with the soluble stroma. However, a fraction of the imported ICS1 protein also partitioned with chloroplast membranes, indicating that ICS1 activity or stability might involve its association with the chloroplast envelope where PHBs most likely reside. ICS1-GFP signals also were visible in the peripheries of chloroplasts, including in stromules (Garcion et al., 2008). In some systems, PHBs play a role in the stabilization of protein complexes. The disruption of mitochondrial PHBs usually destabilizes their interactors and leads to various mitochondrial malfunctions (Van Aken et al., 2007). In yeast, the PHB complex binds to two newly synthesized subunits of respiratory complex IV and protects them against degradation (Steglich et al., 1999; Nijtmans et al., 2000). In Arabidopsis, we demonstrate that disruption of PHB3 function affects ICS1 protein levels without affecting ICS1 RNA accumulation. Therefore, PHB3 may act mainly by stabilizing the ICS1 protein, although it also may affect ICS1 activity. Given the large number of PHBs found in ICS1 complexes, it is possible that several PHBs affect ICS1 and SA production.

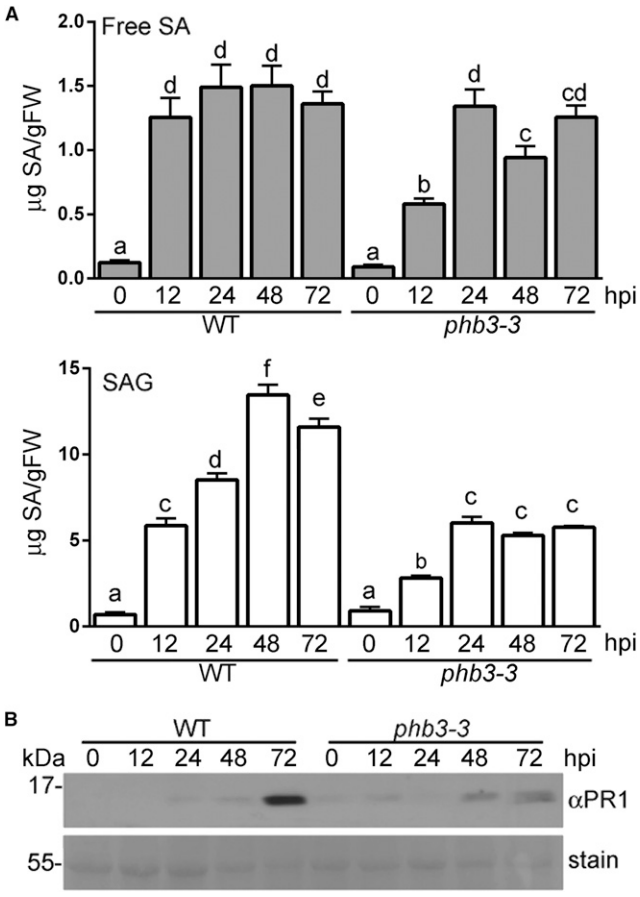

Figure 6. *phb3-3* mutant plants have reduced SA accumulation and PR1 protein levels after infection with *Pst/AvrRpm1*. Two-week-old plants grown on plates were flooded with *Pst/AvrRpm1* bacteria at a concentration of 1×10^6 colony-forming units (CFU) mL^{-1}. Samples were taken at 0, 12, 24, 48, and 72 h post infection (hpi). A, The levels of free SA (gray bars) and glycosylated SA (SAG; white bars) are shown; each bar represents the average of three independent experiments. Error bars indicate SE. Statistical analysis was performed using ANOVA/Fisher's test. Different letters denote statistically significant differences at $P < 0.05$ for free SA and $P < 0.001$ for SAG. B, The levels of PR1 protein were detected by immunoblot analysis using a PR1 antibody. The membrane was stained with Coomassie Blue to show similar protein loading. Similar results were seen in two additional experiments. FW, Fresh weight; WT, wild type.

We focused here on how PHB3 affects ICS1 as well as the downstream production of SA and defense-related signaling outputs such as PR1 and cell death induction. Plants with the *phb3-3* mutation show phenotypes that are distinct from those caused by reduced ICS1/SA levels. In particular, the small-plant phenotype characteristic of *phb3* mutants was not observed in *sid2* plants. The product of ICS1, IC, also is a precursor for phylloquinone, which is barely detectable in the Arabidopsis *sid2ics2* double mutant; this mutant displays a dwarf phenotype similar to *phb3-3*, although the cause of the dwarfism is not known (Garcion et al., 2008). Disruption in the penultimate step in phylloquinone synthesis also results in a modest reduction in plant size (Lohmann et al., 2006). Future work will determine whether PHB3 is required for phylloquinone biosynthesis. It seems possible that the different *phb3-3* mutant phenotypes (reduced size, stress-induced SA and NO) are due to reduced levels of different specific complexes that contain PHB3 in chloroplasts and mitochondria, respectively.

An unanticipated finding resulting from this study is the phenotype of the ICS1-V5-expressing plants, which have very high levels of ICS1 relative to wild-type plants. These plants have only moderately elevated basal SA levels that are increased further in response to UV-C. Why are the SA levels in ICS1-V5 plants low without stress? One possibility is that the upstream chorismate precursor is limiting under basal conditions. This seems unlikely, given that basal chorismate production from the shikimate pathway is usually high (Herrmann and Weaver, 1999). Another possibility is that ICS1 needs activation (e.g. by posttranslational modification[s] or conformational change) or another step required for SA production is limiting.

In conclusion, this work demonstrated that ICS1 is regulated posttranscriptionally by PHB3. During stress or infection, highly increased SA production in Arabidopsis likely requires an increase in ICS1 protein levels. Upon stress, this increase in ICS1 protein levels is produced mainly by transcriptional activation of the *ICS1* gene (Wildermuth et al., 2001; Martínez et al., 2004; Garcion et al., 2008). PHB3 seems to contribute to this process through stabilization of the protein. Whether PHB3 is involved in SA production beyond stabilizing ICS1 will be an interesting topic for future studies.

MATERIALS AND METHODS

Plant Growth Conditions and UV-C Treatments

Arabidopsis (*Arabidopsis thaliana*) wild-type, *phb3-3* (Wang et al., 2010), *sid2-2* (Wildermuth et al., 2001), *sid2-2/ICS1-V5* (transgenic complementation line SM156 in Strawn et al., 2007), *phb3-3/pUBQ:PHB3-V5*, and *phb3-3/p35S:PHB3-GFP* lines (this report) were in the Columbia background. For plants grown in vitro, growth medium contained 0.5× MS medium supplemented with 10 g L^{-1} Suc and 2.6 g L^{-1} Phytagel (Sigma), and plants were incubated in a growth chamber (16 h of light, 100 μmol m^{-2} s^{-1}, 22°C ± 2°C). *Nicotiana benthamiana* plants were grown in soil at 24°C with a 16-h-light/8-h-dark cycle. Fresh spinach (*Spinacia oleracea*) was purchased from a store.

For fractionation and immunoprecipitation experiments, plants were grown in soil in conditions described previously (Pattanayak et al., 2012). Briefly, plants were grown in 50:50 Fafard C2:Metro-Mix soil with a 16-h-light/8-h-dark cycle at 20°C. Otherwise, plants were grown in turba soil mixed with vermiculite 1:1 in a growth room under controlled conditions (16-h-light/8-h-dark cycle, 100 μmol m^{-2} s^{-1}, 22°C ± 2°C).

UV-C treatments for immunoprecipitation of ICS1-V5 complexes and fractionation experiments were performed with 21-d-old wild-type and *sid2-2/ICS1-V5* plants grown in soil by exposing them to 254-nm light from an 18.4-W UVP Mineralight UVGL-55 multiband lamp for 45 min at a distance of 30 cm in a growth chamber. Leaves were collected from untreated plants and from plants 8, 24, and 32 h after UV-C exposure. For UV-C irradiation of in vitro-grown plants (Nawrath and Métraux, 1999), 14-d-old plants were exposed for 20 min in a chamber equipped with two UV-C fluorescent tubes of 8 W each (λ = 254 nm) at a distance of 30 cm above the plates. UV-treated plants were subsequently placed in a growth chamber under controlled conditions for the indicated periods of time.

For SA treatments, 15-d-old seedlings were floated in a solution of 0.5 mM SA in 0.5× MS medium (treatment) or 0.5× MS medium as a control and incubated for the indicated periods of time under continuous light (80 μmol m^{-2} s^{-1}). For immunoblot analysis, whole seedlings were immediately frozen in liquid nitrogen and stored at −80°C until total protein extraction.

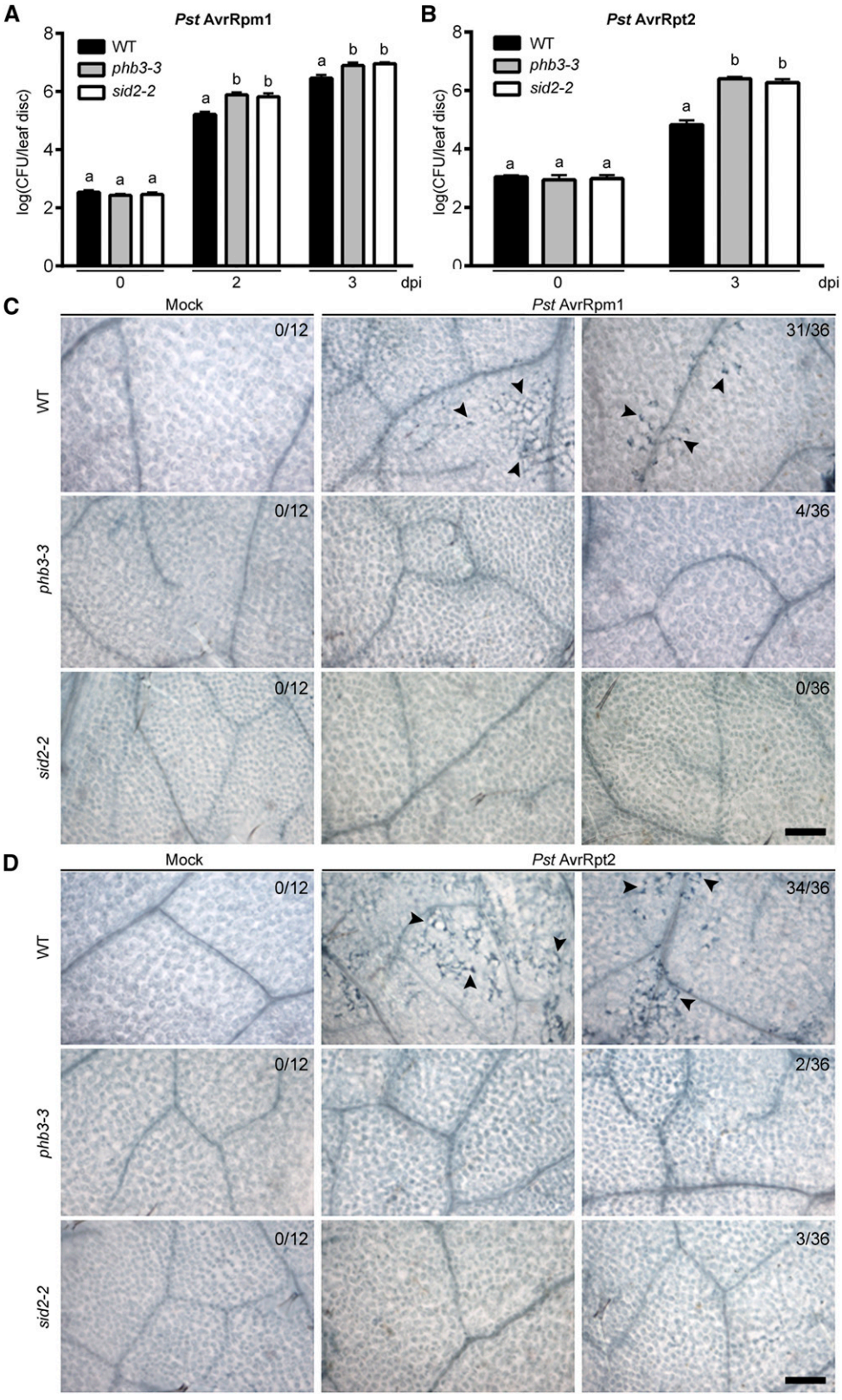

Figure 7. *phb3-3* mutant plants are more susceptible to infection by *Pst* strains DC3000/AvrRpm1 and DC3000/AvrRpt2. A, Two-week-old plate-grown plants were inoculated by flooding the plants with *Pst/AvrRpm1* at a concentration of 1×10^5 CFU mL^{-1}. Bacteria were enumerated at 0, 2, and 3 d post inoculation (dpi). B, Three-week-old plants grown in soil were inoculated with *Pst/AvrRpt2* by infiltration using a concentration of 1×10^5 CFU mL^{-1}. Bacteria were counted at 0 and 3 dpi. For A and B, bars represent average values of 12 replicates; error bars indicate SE. Statistical analysis was performed using ANOVA/Fisher's test. Different letters denote statistically significant differences at P values as follows: A, 2 dpi ($P < 0.0001$) and 3 dpi ($P \leq 0.0005$); B, 3 dpi ($P < 0.0001$). C and D, Cell death was evaluated using Trypan Blue staining in leaf tissue of 4-week-old plants grown in soil 10 h after infiltration with *Pst/AvrRpm1* or *Pst/AvrRpt2* (1×10^8 CFU mL^{-1}). Cell death was scored as occurring if at least six blue-stained cells were visible in the area of tissue shown and if similar staining occurred throughout the inoculated leaf. Numbers indicate the total number of leaves showing cell death out of the total number scored in three independent experiments. Arrowheads indicate examples of the collapsed, Trypan Blue-stained cells. These experiments were repeated three times with similar results. WT, Wild type. Bars = 200 μm.

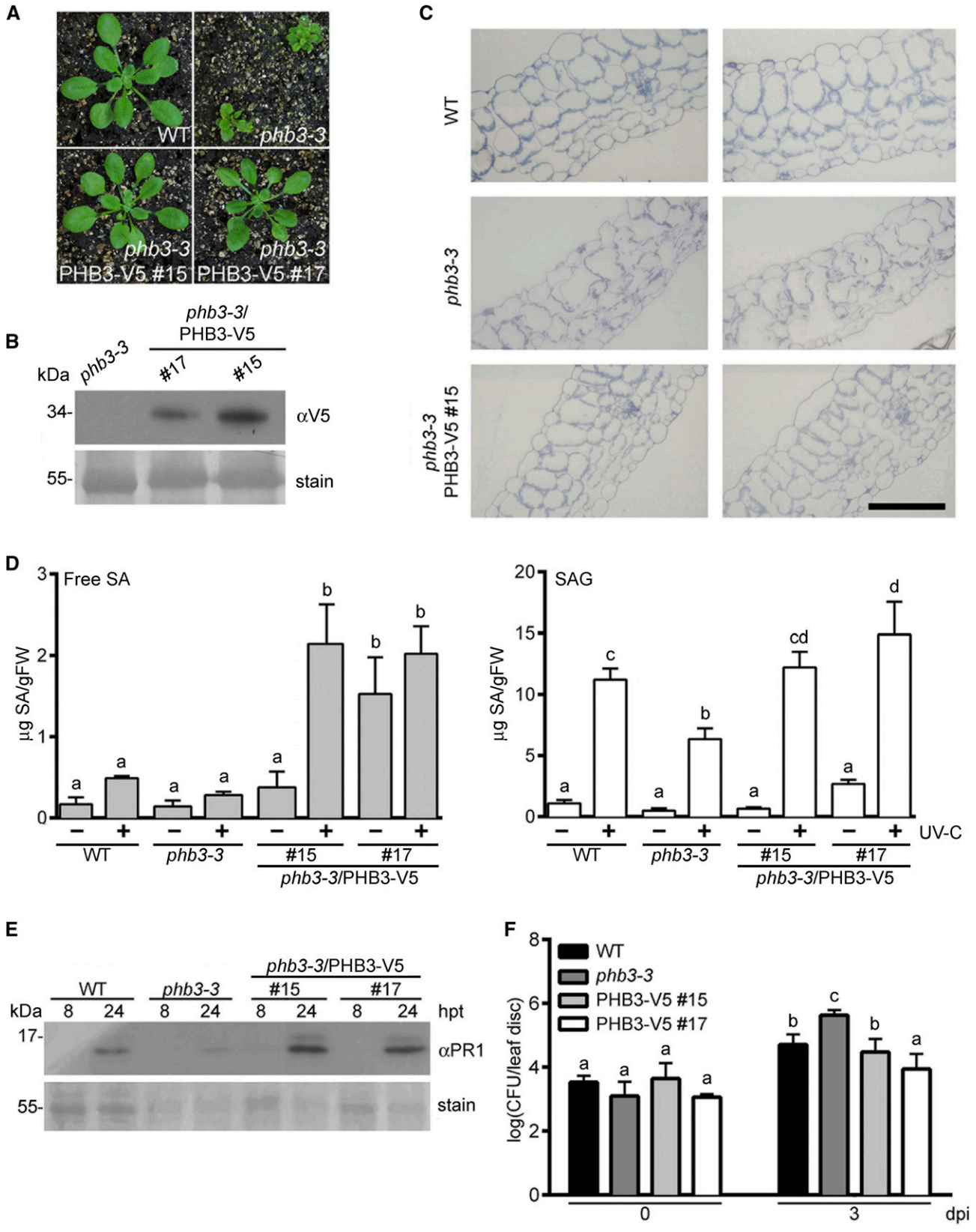

Figure 8. Expression of PHB3 complements *phb3-3* mutant phenotypes. A, Phenotypes of 3-week-old plants grown in soil. B, Immunodetection of the PHB3-V5 protein using V5 antibody in extracts from *phb3-3* and complemented *phb3-3/PHB3-V5* #15 and #17 2-week-old plants grown in soil. C, Leaf cross sections of wild-type (WT), *phb3-3*, and complemented *phb3-3/PHB3-V5*

Bacterial Strains, Plant Inoculation Conditions, Bacterial Proliferation, and Cell Death Assays

Pseudomonas syringae pv *tomato* DC3000 virulent strain and its isogenic avirulent strains expressing the AvrRpm1 (*Pst/AvrRpm1*) or AvrRpt2 (*Pst/AvrRpt2*) effector (Mackey et al., 2002) were used. Bacterial strains were grown at 28°C on King's B medium supplemented with kanamycin at 50 μg mL^{-1}, sedimented by centrifugation, and then resuspended in 10 mM $MgCl_2$. Bacterial inoculation was performed by the flooding of 14-d-old plants (Ishiga et al., 2011) using a suspension of 1×10^6 CFU mL^{-1} (to evaluate SA and PR1 levels) or 1×10^5 CFU mL^{-1} (for bacterial proliferation assays). Alternatively, bacteria were inoculated by syringe infiltration on the abaxial side of the leaves of 4-week-old soil-grown plants (Greenberg et al., 2000) using a suspension of 1×10^5 CFU mL^{-1} (for bacterial proliferation assays) or 1×10^8 CFU mL^{-1} (for cell death assays).

For bacterial proliferation assays, leaf discs from 12 independent inoculated plants were taken at 0, 2, and/or 3 d postinoculation, ground in 10 mM $MgCl_2$, serially diluted 1:10, and plated onto Luria-Bertani agar plates supplemented with 50 μg mL^{-1} kanamycin and 50 μg mL^{-1} rifampicin. Plates were incubated at 28°C for 2 d, and the CFUs were counted manually. Each bacterial proliferation assay was repeated three times.

Cell death was visualized in leaves of 4-week-old soil-grown plants 10 h after bacterial or mock (control) infiltration using Trypan Blue staining (Pavet et al., 2005). Leaves immersed in freshly prepared lactophenol solution (water, basic phenol, lactic acid, and glycerol in a 1:1:1:1 ratio) containing Trypan Blue at 250 μg mL^{-1} were placed in boiling water for 3 min, cleared in lactophenol without Trypan Blue at room temperature for 16 h, mounted in 50% glycerol, and observed using a compound microscope (Nikon Eclipse 80i microscope) at 100× magnification. This experiment was repeated three times. In each experiment, leaves from four independent plants per genotype were analyzed.

Light Microscopy of Leaf Sections

Small slices of the sixth leaf of 3-week-old plants were prepared as described (León et al., 2007). Briefly, samples were fixed overnight in 2.5% (v/v) glutaraldehyde in 0.1 M sodium cacodylate buffer, pH 7, and postfixed in 1% osmium tetroxide for 2 h. Then samples were stained with 1% (w/v) uranyl acetate for 90 min, dehydrated with acetone solutions (50%, 70%, 95%, and 100%), and embedded in Epon resin. Polymerization was performed in a heater at 60°C for 48 h. Fine cuts (80 nm) obtained with a Sorvall MT5000 ultramicrotome were stained with 4% (w/v) uranyl acetate and lead citrate in methanol. Images were taken with a Nikon Eclipse 80i microscope at 40× magnification.

Genetic Constructs and Stable Plant Transformation

To obtain *phb3-3* mutant plants complemented with PHB3, *pUBQ10:PHB3-V5* and *p35S:PHB3-GFP* constructs were generated using Gateway technology following the manufacturer's instructions (Invitrogen). The *PHB3* coding region was obtained by the amplification of cDNA using the primers described in Supplemental Table S2. The PCR fragment was cloned into the pENTR/SD/D-TOPO vector (Invitrogen) and then recombined into the pB7m34gW vector (Karimi et al., 2005) to express the PHB3 protein fused to a V5 tag controlled by the Ubiquitin10 promoter (pUBQ10). For live-imaging experiments of PHB3 fused to the eGFP reporter protein, the amplified PHB3 coding sequence cloned into the pENTR/SD/D-TOPO vector was recombined into the pKGWG2 vector (Karimi et al., 2002).

Final constructs were verified by sequencing and introduced into the *Agrobacterium tumefaciens* C58 strain. Stable Arabidopsis *phb3-3* transformants were obtained using the floral dip method (Zhang et al., 2006). Transgenic seeds were selected in 0.5× MS solid medium supplemented with 50 μg mL^{-1} kanamycin for the GFP reporter lines or with 15 μg mL^{-1} glufosinate-ammonium for the PHB3-V5-expressing lines. Homozygous transgenic lines were selected and used for further analyses.

Protein Extracts, Immunoblot, and Immunoprecipitation

Total protein extracts were obtained from wild-type and transgenic lines by homogenizing 0.5 g of tissue (each sample was composed of 12–15 seedlings grown on plates or several mature leaves of plants grown in soil) per 1 mL of extraction buffer (50 mM sodium phosphate buffer, pH 8, 150 mM NaCl, 0.2% Igepal, 5 mM EDTA, and 1× complete Protease Inhibitor Cocktail solution [Roche Diagnostics]). After centrifugation at 2,350*g* for 10 min, supernatants were transferred to clean tubes and stored at –80°C. Protein concentration was determined by the Bradford method using the Bio-Rad Protein Assay (Bio-Rad Laboratories).

For immunoblot analysis, total or chloroplast (see below) protein extracts (30 μg of protein per lane) were separated on 12% SDS-PAGE gels and transferred to Immobilon PDVF membranes (Millipore) by semidry electroblotting. The membranes were blocked for 1 h in PBS solution (PBS-T: 137 mM NaCl, 2.7 mM KCl, 10 mM Na_2HPO_4, 2 mM KH_2PO_4, and 0.1% Tween 20) with 5% nonfat dried milk at room temperature. To detect the ICS1-V5 and PHB3-V5 fusion proteins, the mouse monoclonal V5 antibody (Invitrogen; R96025) was used at a 1:5,000 dilution. To detect PR1, the rabbit polyclonal PR1 antibody (Agrisera; AS10 687) was used at a 1:2,500 dilution. PHBs were detected with the PHB3/4 rabbit polyclonal antibody described previously (Snedden and Fromm, 1997; Van Aken et al., 2007) at a 1:10,000 dilution.

ICS1 was detected with the rabbit polyclonal ICS1 antibody UCB68 at a 1:10,000 dilution. This antibody was made by immunizing rabbits with purified recombinant mature ICS1 protein (described by Strawn et al. [2007]). The titer and specificity of the antibody were tested by immunoblot analysis. The antibody can detect as low as 31 pg of recombinant ICS1 protein, with ready detection of ICS1 protein in UV-C-induced leaf extracts using a 1:10,000 dilution.

Proteins used as markers for subcellular localization were detected using rabbit polyclonal antibodies against AtpB (chloroplast, 1:10,000; a gift from Dr. Dominique Drapier [Drapier et al., 2007]), Prx IIF (mitochondria, 1:3,000; a gift from Dr. Karl-Josef Dietz [Finkemeier et al., 2005]), cFBPase (cytoplasm, 1:25,000; Agrisera; AS04043), H^+-ATPase (plasma membrane, 1:2,000; Agrisera; AS07260), Tic110 (chloroplast inner envelope, 1:3,000; a gift from Masato Nakai [Kikuchi et al., 2006]), NOA1 (1:10,000; a gift from Pradeep Kachroo [Mandal et al., 2012]), LOX-C (1:30,000; Agrisera; AS07258), LHCII (thylakoid, 1:5,000; a gift from Roberto Bassi [Di Paolo et al., 1990]), SFR2 N and C (chloroplast outer envelope, 1:1,000; a gift from Christoph Benning [Roston et al., 2014]), and a guinea pig antibody against chloroplast Hsp70 (1:12,000; a gift from Thomas Leustek [Wang et al., 1993]).

After washing in PBS-T (three times), the membranes were incubated with the anti-mouse horseradish peroxidase-conjugated secondary antibody (KPL [074-1806], 1:10,000 and Thermo Fisher [31440], 1:1,000), anti-guinea pig peroxidase antibody (Sigma [A5545], 1:100,000), or the anti-rabbit horseradish antibody (Invitrogen [65-6120], 1:10,000 and Thermo Fisher [32460], 1:1,000). After washing in PBS-T (15 min three times), proteins immunodetected were visualized using chemiluminescence kits (Thermo Fisher Scientific [34087 and 34095]) according to the manufacturer's instructions.

Figure 8. (*Continued.*)
#15 plants. Bar = 100 μm. D, Levels of free SA (gray bars) and glycosylated SA (SAG; white bars) in plants grown on plates, treated with UV-C light for 20 min, and harvested at 24 h post treatment (+). Untreated plants were used as controls (–). SA levels are expressed as μg g^{-1} fresh weight (FW). Each bar represents the mean value of three independent experiments; error bars indicate SE. Statistical analysis was performed using ANOVA/Fisher's test. Different letters denote statistically significant differences at $P < 0.02$ for free SA and $P < 0.04$ for SAG. E, PR1 protein was detected by immunoblot using PR1 antibody in wild-type, *phb3-3*, and *phb3-3/PHB3-V5* complemented line plants grown on plates, treated with UV-C light for 20 min, then harvested at 8 and 24 h post treatment (hpt). The gel shows a representative result from three independent experiments. F, Bacterial proliferation was quantified in 3-week-old plants grown in soil at 0 and 3 dpi with 1×10^5 CFU mL^{-1} *Pst/AvrRpt2*. Each bar represents the average of 12 replicates; error bars indicate SE. Statistical analysis was performed using ANOVA/Fisher's test. Different letters denote statistically significant differences at $P < 0.05$. This experiment was repeated three times with similar results. In B and E, membranes were stained with Coomassie Blue to show similar protein loading.

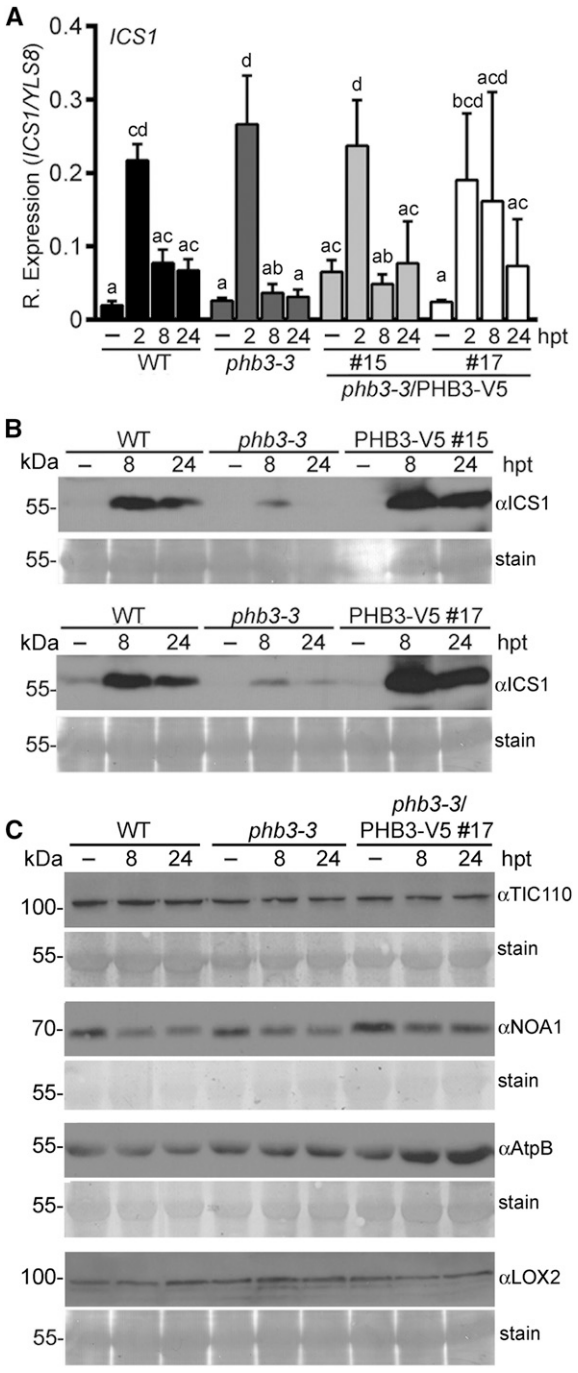

Figure 9. PHB3 regulates ICS1 protein levels. A, *ICS1* transcript levels measured by RT-qPCR in 2-week-old plants grown on plates and treated with UV-C light for 20 min. Whole seedlings were harvested at 2, 8, and 24 h post treatment (hpt). – indicates untreated plants. *ICS1* transcript levels are relative (R.) to *YLS8*, which was used as an endogenous control. Bars show means of three biological replicates; error bars show SE. Statistical analysis was performed using ANOVA/Fisher's test. Different letters denote statistically significant differences at $P < 0.05$. B, ICS1 was detected by immunoblot analysis with ICS1 antibody in extracts of plants treated as in A. C, PHB3 does not affect other chloroplast protein levels. The chloroplast proteins Tic110, NOA1, AtpB, and LOX2 were detected by immunoblot analysis with specific antibodies. Representative data from three (B) or two (C) independent experiments are shown. Coomassie Blue (B) and Ponceau S (C) staining of proteins in the membranes show similar loading. The LOX2 immunoblot shows the same membrane as the ICS1 blot in B (bottom). WT, Wild type.

All immunoblots were repeated two or three times with new samples, as indicated in the corresponding figure legends.

For immunoprecipitation of ICS1-V5-containing complexes, total protein extracts of untreated and UV-C-treated wild-type and *sid2-2/ICS1-V5* plants (see above) were prepared as described (Jelenska et al., 2010). Immunoprecipitation was performed using anti-V5 agarose (Sigma; A7345). After immunoprecipitation, proteins were separated by SDS-PAGE and analyzed either by Coomassie Blue staining and LC-MS/MS or by immunoblotting. This experiment was repeated three times with different protein extract samples.

Database Searching of Peptides Identified by LC-MS/MS

LC-MS/MS protein identification was performed at the Stanford University Mass Spectrometry Facility. Protein bands in ICS1-V5 immunoprecipitations and the corresponding regions of wild-type samples were cut from the gel; UV-C-treated and untreated samples were combined for further analysis. Proteins in gel bands were digested with trypsin and extracted, and peptides were identified as described (Jelenska et al., 2010). MS/MS samples were analyzed using Sequest (version 27, rev. 11; Thermo Fisher Scientific) set up to search the National Center for Biotechnology Information Arabidopsis database (222,041 entries) assuming the digestion enzyme stricttrypsin. Scaffold (version Scaffold_3.1.4.1; Proteome Software) was used to validate MS/MS-based identifications of peptides (at greater than 95% probability) and proteins (at greater than 95% probability and containing at least one identified peptide).

Chloroplast Isolation, Fractionation, and Thermolysin Treatment

Three-week-old wild-type and *sid2-2/ICS1-V5* plants grown in soil were treated with UV-C, and chloroplasts were isolated in a Percoll gradient as described (Kubis et al., 2008). The purity of the chloroplast fractions was evaluated by immunoblot analysis as described above. *N. benthamiana* chloroplasts were isolated and treated with thermolysin (Sigma) according to Lamppa (1995). Arabidopsis chloroplasts for the thermolysin treatment experiment were isolated as described (Aronsson and Jarvis, 2002). For membrane association, spinach, *N. benthamiana*, and Arabidopsis chloroplasts were isolated as described (Kieselbach et al., 1998) and partitioned to membrane and soluble fractions according to Lamppa (1995).

Confocal Microscopy

Leaves and cotyledons of ~10-d-old seedlings of *phb3-3/PHB3-GFP* (line 6.5) Arabidopsis were used for imaging. *N. benthamiana* plants grown in soil were transiently transformed with agrobacteria harboring the constructs *p35S:PHB3-GFP* (see above), *pdex:OEP7-RFP* (Cecchini et al., 2015), *pd35S:COX4-mCherry* (mt-rb; Nelson et al., 2007), and *p35S:COX4-dsRed* (from Dr. Guo-Liang Wang [Li et al., 2017]) as described (Cecchini et al., 2015; Jelenska et al., 2017). Agrobacteria with different constructs were infiltrated together, and *N. benthamiana* leaves were imaged 2 d later. Leaves transformed with the *pdex:OEP7-RFP* construct were sprayed with 3 μM dexamethasone 1 d after agroinfiltration. Three-week-old *N. benthamiana* plants were used for images with mitochondrial markers, and 5- to 6-week-old plants were used for other images.

Confocal images were obtained using a Zeiss LSM710 laser-scanning confocal microscope as described (Kang et al., 2014; Cecchini et al., 2015; Jelenska et al., 2017). Fluorescence was visualized as follows: GFP, excitation 488 nm/emission 496 to 557 nm; RFP, excitation 561/emission 570 to 619 nm; mCherry/dsRed, excitation 561 nm/emission 580 to 629 nm; and chlorophyll autofluorescence, excitation 633 nm/emission 655 to 747 nm. Fluorescence in different channels was acquired for the same field using a sequential acquisition mode for PHB3 + OEP7 and simultaneously for PHB3 + COX4 to allow the imaging of moving mitochondria. Z series images (14–18 μm for *N. benthamiana* and 21 μm for Arabidopsis) and time series videos (60-image series) were processed with ImageJ (https://imagej.nih.gov/ij).

Quantitation of SA

Free SA and glycosylated SA extracted from leaf tissues were quantified by HPLC using an Atlantis T3 column, as described previously (Verberne et al., 2002). The results show data from three independent experiments. Each sample consisted of 0.5 g of tissue collected from a pool of 12 to 15 seedlings grown on plates or mature leaves from three plants grown in soil.

RT-qPCR Analysis

Whole UV-C-treated plants (four seedlings per genotype) grown in vitro were frozen in liquid nitrogen and stored at −80°C until RNA isolation. Total RNA was obtained from frozen samples using TRIzol Reagent (Invitrogen) according to the manufacturer's instructions. cDNA was synthesized from each sample (2 μg of total RNA) with an ImProm II Kit (Promega). qPCR was performed using the Brilliant III Ultra-Fast SYBR Green QPCR Master Mix (Agilent Technologies) reagents on AriaMx real-time PCR system equipment. The expression levels of the *ICS1* gene were calculated relative to the *YLS8* endogenous control. Primers used for each gene are listed in Supplemental Table S2. The data represent results from three biological replicates (independent experiments). In each experiment, three technical replicates from the same cDNA sample were used.

Accession Numbers

Sequence data from this article are found in the GenBank/EMBL data libraries under the following accession numbers: for Arabidopsis, AT1G74710 (ICS1/SID2), AT5G40770 (PHB3), AT1G03860 (PHB2), AT3G27280 (PHB4), AT2G20530 (PHB6), AT4G28510 (PHB1), AT2G14610 (PR1), AT5G08290 (YLS8), AT3G52420 (OEP7), AT3G06050 (PRX IIF), AT1G43670 (cFBPase), AT4G30190 (H^+-ATPase), AT1G06950 (TIC110), AT4G24280 (cpHSP70-1), AT5G49910 (cpHSP70-2), AT3G06510 (SFR2), ATCG00480 (AtpB), AT3G47450 (NOA1), and AT3G45140 (LOX2); for *Saccharomyces cerevisiae*, YGL187C (ScCOX4); for *N. benthamiana*, DQ121387 (NbPHB1) and DQ121388 (NbPHB2); and for spinach, AF035456, AF039083, M99565 (So-cpHSP70s), and 2715576 (SoAtpB).

Supplemental Data

The following supplemental materials are available.

Supplemental Figure S1. Spectrum counts of peptides detected by LC-MS/MS in wild-type and *sid2-2/ICS1-V5* samples.

Supplemental Figure S2. PHB3/4 protein levels in UV-C-treated wild-type, *phb3-3*, and *phb3-3/PHB3-V5* plants.

Supplemental Figure S3. PHB3 colocalizes with chloroplasts and mitochondrial markers.

Supplemental Table S1. List of peptides matching PHB protein family members and ICS1 and the number of spectra of peptides found from the top enriched proteins identified in ICS1-V5 complexes by LC-MS/MS analysis.

Supplemental Table S2. List of primers.

Supplemental Video S1. Video of *N. benthamiana* leaves expressing PHB3-GFP.

Supplemental Video S2. Video of *N. benthamiana* leaves expressing PHB3-GFP and mitochondrial marker COX4-mCherry.

ACKNOWLEDGMENTS

We thank Hillel Fromm (Tel Aviv University) for providing the PHB3/4 antibody, Dominique Drapier (Centre National de la Recherche Scientifique/UPMC) for the AtpB antibody, Karl-Josef Dietz (Bielefeld University) for the Prx IIF antibody, Pradeep Kachroo (University of Kentucky) for the NOA1 antibody, Gopal Pattanayak (University of Chicago) for antibodies against Tic110 (from Masato Nakai, Osaka University) and LHCII (from Roberto Bassi, Università di Verona), Thomas Leustek (Rutgers University) for the cpHSP70 antibody, Christoph Benning (Michigan State University) for the SFR2 antibody, Andreas Nebenführ (University of Tennessee) for the *COX4-mCherry* marker, and Guo-Liang Wang (Ohio State University) for the *COX4-dsRed* marker. We also thank Jacquelyn Freeman for help with immunoprecipitation experiments and Michael Allara for help with western blots.

Received July 13, 2017; accepted January 22, 2018; published February 1, 2018.

LITERATURE CITED

Abreu ME, Munné-Bosch S (2009) Salicylic acid deficiency in NahG transgenic lines and *sid2* mutants increases seed yield in the annual plant *Arabidopsis thaliana*. J Exp Bot **60:** 1261–1271

Ahn CS, Lee JH, Reum Hwang A, Kim WT, Pai HS (2006) Prohibitin is involved in mitochondrial biogenesis in plants. Plant J **46:** 658–667

Aronsson H, Jarvis P (2002) A simple method for isolating import-competent Arabidopsis chloroplasts. FEBS Lett **529:** 215–220

Beckers GJM, Jaskiewicz M, Liu Y, Underwood WR, He SY, Zhang S, Conrath U (2009) Mitogen-activated protein kinases 3 and 6 are required for full priming of stress responses in *Arabidopsis thaliana*. Plant Cell **21:** 944–953

Brodersen P, Malinovsky FG, Hématy K, Newman MA, Mundy J (2005) The role of salicylic acid in the induction of cell death in Arabidopsis *acd11*. Plant Physiol **138:** 1037–1045

Cao H, Glazebrook J, Clarke JD, Volko S, Dong X (1997) The Arabidopsis *NPR1* gene that controls systemic acquired resistance encodes a novel protein containing ankyrin repeats. Cell **88:** 57–63

Catinot J, Buchala A, Abou-Mansour E, Métraux JP (2008) Salicylic acid production in response to biotic and abiotic stress depends on isochorismate in *Nicotiana benthamiana*. FEBS Lett **582:** 473–478

Cecchini NM, Steffes K, Schläppi MR, Gifford AN, Greenberg JT (2015) Arabidopsis AZI1 family proteins mediate signal mobilization for systemic defence priming. Nat Commun **6:** 7658

Chen H, Xue L, Chintamanani S, Germain H, Lin H, Cui H, Cai R, Zuo J, Tang X, Li X, et al (2009) ETHYLENE INSENSITIVE3 and ETHYLENE INSENSITIVE3-LIKE1 repress *SALICYLIC ACID INDUCTION DEFICIENT2* expression to negatively regulate plant innate immunity in *Arabidopsis*. Plant Cell **21:** 2527–2540

Christians MJ, Larsen PB (2007) Mutational loss of the prohibitin AtPHB3 results in an extreme constitutive ethylene response phenotype coupled with partial loss of ethylene-inducible gene expression in Arabidopsis seedlings. J Exp Bot **58:** 2237–2248

Clarke SM, Cristescu SM, Miersch O, Harren FJM, Wasternack C, Mur LAJ (2009) Jasmonates act with salicylic acid to confer basal thermotolerance in *Arabidopsis thaliana*. New Phytol **182:** 175–187

Clarke SM, Mur LAJ, Wood JE, Scott IM (2004) Salicylic acid dependent signaling promotes basal thermotolerance but is not essential for acquired thermotolerance in *Arabidopsis thaliana*. Plant J **38:** 432–447

Coll NS, Epple P, Dangl JL (2011) Programmed cell death in the plant immune system. Cell Death Differ **18:** 1247–1256

Cui H, Gobbato E, Kracher B, Qiu J, Bautor J, Parker JE (2017) A core function of EDS1 with PAD4 is to protect the salicylic acid defense sector in Arabidopsis immunity. New Phytol **213:** 1802–1817

Delaney TP, Uknes S, Vernooij B, Friedrich L, Weymann K, Negrotto D, Gaffney T, Gut-Rella M, Kessmann H, Ward E, et al (1994) A central role of salicylic acid in plant disease resistance. Science **266:** 1247–1250

Dempsey DA, Vlot AC, Wildermuth MC, Klessig DF (2011) Salicylic acid biosynthesis and metabolism. The Arabidopsis Book **9:** e0156,

Dewdney J, Reuber TL, Wildermuth MC, Devoto A, Cui J, Stutius LM, Drummond EP, Ausubel FM (2000) Three unique mutants of Arabidopsis identify *eds* loci required for limiting growth of a biotrophic fungal pathogen. Plant J **24:** 205–218

Ding Y, Shaholli D, Mou Z (2015) A large-scale genetic screen for mutants with altered salicylic acid accumulation in Arabidopsis. Front Plant Sci **5:** 763

Di Paolo ML, Dal Belin Peruffo A, Bassi R (1990) Immunological studies on chlorophyll-a/b proteins and their distribution in thylakoid membrane domains. Planta **181:** 275–286

Drapier D, Rimbault B, Vallon O, Wollman FA, Choquet Y (2007) Intertwined translational regulations set uneven stoichiometry of chloroplast ATP synthase subunits. EMBO J **26:** 3581–3591

Finkemeier I, Goodman M, Lamkemeyer P, Kandlbinder A, Sweetlove LJ, Dietz KJ (2005) The mitochondrial type II peroxiredoxin F is

essential for redox homeostasis and root growth of *Arabidopsis thaliana* under stress. J Biol Chem **280:** 12168–12180

Fragnière C, Serrano M, Abou-Mansour E, Métraux JP, L'Haridon F (2011) Salicylic acid and its location in response to biotic and abiotic stress. FEBS Lett **585:** 1847–1852

Fu ZQ, Dong X (2013) Systemic acquired resistance: turning local infection into global defense. Annu Rev Plant Biol **64:** 839–863

Fu ZQ, Yan S, Saleh A, Wang W, Ruble J, Oka N, Mohan R, Spoel SH, Tada Y, Zheng N, et al (2012) NPR3 and NPR4 are receptors for the immune signal salicylic acid in plants. Nature **486:** 228–232

Garcion C, Lohmann A, Lamodière E, Catinot J, Buchala A, Doermann P, Métraux JP (2008) Characterization and biological function of the *ISOCHORISMATE SYNTHASE2* gene of Arabidopsis. Plant Physiol **147:** 1279–1287

Greenberg JT, Silverman FP, Liang H (2000) Uncoupling salicylic acid-dependent cell death and defense-related responses from disease resistance in the Arabidopsis mutant *acd5*. Genetics **156:** 341–350

Guo B, Liu C, Li H, Yi K, Ding N, Li N, Lin Y, Fu Q (2016) Endogenous salicylic acid is required for promoting cadmium tolerance of Arabidopsis by modulating glutathione metabolisms. J Hazard Mater **316:** 77–86

Hardré H, Kuhn L, Albrieux C, Jouhet J, Michaud M, Seigneurin-Berny D, Falconet D, Block MA, Maréchal E (2014) The selective biotin tagging and thermolysin proteolysis of chloroplast outer envelope proteins reveals information on protein topology and association into complexes. Front Plant Sci **5:** 203

Herrmann KM, Weaver LM (1999) The shikimate pathway. Annu Rev Plant Physiol Plant Mol Biol **50:** 473–503

Huang J, Gu M, Lai Z, Fan B, Shi K, Zhou YH, Yu JQ, Chen Z (2010) Functional analysis of the Arabidopsis PAL gene family in plant growth, development, and response to environmental stress. Plant Physiol **153:** 1526–1538

Ichimura K, Casais C, Peck SC, Shinozaki K, Shirasu K (2006) MEKK1 is required for MPK4 activation and regulates tissue-specific and temperature-dependent cell death in Arabidopsis. J Biol Chem **281:** 36969–36976

Inaba T, Li M, Alvarez-Huerta M, Kessler F, Schnell DJ (2003) atTic110 functions as a scaffold for coordinating the stromal events of protein import into chloroplasts. J Biol Chem **278:** 38617–38627

Ishiga Y, Ishiga T, Uppalapati SR, Mysore KS (2011) Arabidopsis seedling flood-inoculation technique: a rapid and reliable assay for studying plant-bacterial interactions. Plant Methods **7:** 32

Jackson DT, Froehlich JE, Keegstra K (1998) The hydrophilic domain of Tic110, an inner envelope membrane component of the chloroplastic protein translocation apparatus, faces the stromal compartment. J Biol Chem **273:** 16583–16588

Jelenska J, Davern SM, Standaert RF, Mirzadeh S, Greenberg JT (2017) Flagellin peptide flg22 gains access to long-distance trafficking in Arabidopsis via its receptor, FLS2. J Exp Bot **68:** 1769–1783

Jelenska J, van Hal JA, Greenberg JT (2010) *Pseudomonas syringae* hijacks plant stress chaperone machinery for virulence. Proc Natl Acad Sci USA **107:** 13177–13182

Kang Y, Jelenska J, Cecchini NM, Li Y, Lee MW, Kovar DR, Greenberg JT (2014) HopW1 from *Pseudomonas syringae* disrupts the actin cytoskeleton to promote virulence in Arabidopsis. PLoS Pathog **10:** e1004232

Karimi M, De Meyer B, Hilson P (2005) Modular cloning in plant cells. Trends Plant Sci **10:** 103–105

Karimi M, Inzé D, Depicker A (2002) GATEWAY vectors for Agrobacterium-mediated plant transformation. Trends Plant Sci **7:** 193–195

Kieselbach T, Hagman, Andersson B, Schröder WP (1998) The thylakoid lumen of chloroplasts: isolation and characterization. J Biol Chem **273:** 6710–6716

Kikuchi S, Hirohashi T, Nakai M (2006) Characterization of the preprotein translocon at the outer envelope membrane of chloroplasts by blue native PAGE. Plant Cell Physiol **47:** 363–371

Kim HS, Desveaux D, Singer AU, Patel P, Sondek J, Dangl JL (2005) The *Pseudomonas syringae* effector AvrRpt2 cleaves its C-terminally acylated target, RIN4, from Arabidopsis membranes to block RPM1 activation. Proc Natl Acad Sci USA **102:** 6496–6501

Kleffmann T, Russenberger D, von Zychlinski A, Christopher W, Sjölander K, Gruissem W, Baginsky S (2004) The *Arabidopsis thaliana* chloroplast proteome reveals pathway abundance and novel protein functions. Curr Biol **14:** 354–362

Kubis SE, Lilley KSJP, Jarvis P (2008) Isolation and preparation of chloroplasts from *Arabidopsis thaliana* plants. Methods Mol Biol **425:** 171–186

Lamppa GK (1995) In vitro import of proteins into chloroplasts. *In* P Maliga, DF Klessig, AR Cashmore, W Gruissem, JE Varner, eds, Methods in Plant Molecular Biology. Cold Spring Harbor Laboratory Press, Cold Spring Harbor, NY, pp 141–171

Lee J, Lee H, Kim J, Lee S, Kim DH, Kim S, Hwang I (2011) Both the hydrophobicity and a positively charged region flanking the C-terminal region of the transmembrane domain of signal-anchored proteins play critical roles in determining their targeting specificity to the endoplasmic reticulum or endosymbiotic organelles in *Arabidopsis* cells. Plant Cell **23:** 1588–1607

Lee MW, Lu H, Jung HW, Greenberg JT (2007) A key role for the *Arabidopsis* WIN3 protein in disease resistance triggered by *Pseudomonas syringae* that secrete AvrRpt2. Mol Plant Microbe Interact **20:** 1192–1200

Lee S, Kim SG, Park CM (2010) Salicylic acid promotes seed germination under high salinity by modulating antioxidant activity in Arabidopsis. New Phytol **188:** 626–637

León G, Holuigue L, Jordana X (2007) Mitochondrial complex II is essential for gametophyte development in Arabidopsis. Plant Physiol **143:** 1534–1546

Li Z, Ding B, Zhou X, Wang GL (2017) The rice dynamin-related protein OsDRP1E negatively regulates programmed cell death by controlling the release of cytochrome c from mitochondria. PLoS Pathog **13:** e1006157

Lohmann A, Schöttler MA, Bréhélin C, Kessler F, Bock R, Cahoon EB, Dörmann P (2006) Deficiency in phylloquinone (vitamin K1) methylation affects prenyl quinone distribution, photosystem I abundance, and anthocyanin accumulation in the Arabidopsis *AtmenG* mutant. J Biol Chem **281:** 40461–40472

Lu H (2009) Dissection of salicylic acid-mediated defense signaling networks. Plant Signal Behav **4:** 713–717

Lu H, Rate DN, Song JT, Greenberg JT (2003) ACD6, a novel ankyrin protein, is a regulator and an effector of salicylic acid signaling in the *Arabidopsis* defense response. Plant Cell **15:** 2408–2420

Macaulay KM, Heath GA, Ciulli A, Murphy AM, Abell C, Carr JP, Smith AG (2017) The biochemical properties of the two Arabidopsis thaliana isochorismate synthases. Biochem J **474:** 1579–1590

Mackey D, Holt BF III, Wiig A, Dangl JL (2002) RIN4 interacts with *Pseudomonas syringae* type III effector molecules and is required for RPM1-mediated resistance in Arabidopsis. Cell **108:** 743–754

Mandal MK, Chandra-Shekara AC, Jeong RD, Yu K, Zhu S, Chanda B, Navarre D, Kachroo A, Kachroo P (2012) Oleic acid-dependent modulation of NITRIC OXIDE ASSOCIATED1 protein levels regulates nitric oxide-mediated defense signaling in *Arabidopsis*. Plant Cell **24:** 1654–1674

Martínez C, Pons E, Prats G, León J (2004) Salicylic acid regulates flowering time and links defence responses and reproductive development. Plant J **37:** 209–217

Mateo A, Funck D, Mühlenbock P, Kular B, Mullineaux PM, Karpinski S (2006) Controlled levels of salicylic acid are required for optimal photosynthesis and redox homeostasis. J Exp Bot **57:** 1795–1807

Mauch F, Mauch-Mani B, Gaille C, Kull B, Haas D, Reimmann C (2001) Manipulation of salicylate content in *Arabidopsis thaliana* by the expression of an engineered bacterial salicylate synthase. Plant J **25:** 67–77

Morris K, MacKerness SA, Page T, John CF, Murphy AM, Carr JP, Buchanan-Wollaston V (2000) Salicylic acid has a role in regulating gene expression during leaf senescence. Plant J **23:** 677–685

Nawrath C, Heck S, Parinthawong N, Métraux JP (2002) EDS5, an essential component of salicylic acid-dependent signaling for disease resistance in *Arabidopsis*, is a member of the MATE transporter family. Plant Cell **14:** 275–286

Nawrath C, Métraux JP (1999) Salicylic acid induction-deficient mutants of *Arabidopsis* express PR-2 and PR-5 and accumulate high levels of camalexin after pathogen inoculation. Plant Cell **11:** 1393–1404

Nelson BK, Cai X, Nebenführ A (2007) A multicolored set of in vivo organelle markers for co-localization studies in Arabidopsis and other plants. Plant J **51:** 1126–1136

Nijtmans LG, de Jong L, Artal Sanz M, Coates PJ, Berden JA, Back JW, Muijsers AO, van der Spek H, Grivell LA (2000) Prohibitins act as a

membrane-bound chaperone for the stabilization of mitochondrial proteins. EMBO J **19:** 2444–2451

Nomura H, Komori T, Uemura S, Kanda Y, Shimotani K, Nakai K, Furuichi T, Takebayashi K, Sugimoto T, Sano S, et al (2012) Chloroplast-mediated activation of plant immune signalling in Arabidopsis. Nat Commun **3:** 926

Nugroho LH, Verberne MC, Verpoorte R (2001) Salicylic acid produced by isochorismate synthase and isochorismate pyruvate lyase in various parts of constitutive salicylic acid producing tobacco plants. Plant Sci **161:** 911–915

Ogawa D, Nakajima N, Sano T, Tamaoki M, Aono M, Kubo A, Kanna M, Ioki M, Kamada H, Saji H (2005) Salicylic acid accumulation under O_3 exposure is regulated by ethylene in tobacco plants. Plant Cell Physiol **46:** 1062–1072

Okrent RA, Brooks MD, Wildermuth MC (2009) Arabidopsis GH3.12 (PBS3) conjugates amino acids to 4-substituted benzoates and is inhibited by salicylate. J Biol Chem **284:** 9742–9754

Pattanayak GK, Venkataramani S, Hortensteiner S, Kunz L, Christ B, Moulin M, Smith AG, Okamoto Y, Tamiaki H, Sugishima M, et al (2012) Accelerated cell death 2 suppresses mitochondrial oxidative bursts and modulates cell death in Arabidopsis. Plant J **69:** 589–600

Pavet V, Olmos E, Kiddle G, Mowla S, Kumar S, Antoniw J, Alvarez ME, Foyer CH (2005) Ascorbic acid deficiency activates cell death and disease resistance responses in Arabidopsis. Plant Physiol **139:** 1291–1303

Piechota J, Bereza M, Sokołowska A, Suszyn K, Lech K, Jan H (2015) Unraveling the functions of type II-prohibitins in Arabidopsis mitochondria. Plant Mol Biol **1:** 249–267

Piechota J, Kolodziejczak M, Juszczak I, Sakamoto W, Janska H (2010) Identification and characterization of high molecular weight complexes formed by matrix AAA proteases and prohibitins in mitochondria of *Arabidopsis thaliana*. J Biol Chem **285:** 12512–12521

Poulsen C, Verpoorte R (1991) Roles of chorismate mutase, isochorismate synthase and anthranilate synthase in plants. Phytochemistry **30:** 377–386

Raskin I, Ehmann A, Melander WR, Meeuse BJ (1987) Salicylic acid: a natural inducer of heat production in *Arum* lilies. Science **237:** 1601–1602

Roston RL, Wang K, Kuhn LA, Benning C (2014) Structural determinants allowing transferase activity in SENSITIVE TO FREEZING 2, classified as a family I glycosyl hydrolase. J Biol Chem **289:** 26089–26106

Schmid J, Amrhein N (1995) Molecular organization of the shikimate pathway in higher plants. Phytochemistry **39:** 737–749

Serrano M, Wang B, Aryal B, Garcion C, Abou-Mansour E, Heck S, Geisler M, Mauch F, Nawrath C, Métraux JP (2013) Export of salicylic acid from the chloroplast requires the multidrug and toxin extrusion-like transporter EDS5. Plant Physiol **162:** 1815–1821

Shapiro AD, Zhang C (2001) The role of NDR1 in avirulence gene-directed signaling and control of programmed cell death in Arabidopsis. Plant Physiol **127:** 1089–1101

Shine MB, Yang JW, El-Habbak M, Nagyabhyru P, Fu DQ, Navarre D, Ghabrial S, Kachroo P, Kachroo A (2016) Cooperative functioning between phenylalanine ammonia lyase and isochorismate synthase activities contributes to salicylic acid biosynthesis in soybean. New Phytol **212:** 627–636

Simoh S, Linthorst HJM, Lefeber AWM, Erkelens C, Kim HK, Choi YH, Verpoorte R (2010) Metabolic changes of *Brassica rapa* transformed with a bacterial isochorismate synthase gene. J Plant Physiol **167:** 1525–1532

Snedden WA, Fromm H (1997) Characterization of the plant homologue of prohibitin, a gene associated with antiproliferative activity in mammalian cells. Plant Mol Biol **33:** 753–756

Song JT, Lu H, Greenberg JT (2004) Divergent roles in *Arabidopsis thaliana* development and defense of two homologous genes, *aberrant growth and death2* and *AGD2-LIKE DEFENSE RESPONSE PROTEIN1*, encoding novel aminotransferases. Plant Cell **16:** 353–366

Steglich G, Neupert W, Langer T (1999) Prohibitins regulate membrane protein degradation by the m-AAA protease in mitochondria. Mol Cell Biol **19:** 3435–3442

Strawn MA, Marr SK, Inoue K, Inada N, Zubieta C, Wildermuth MC (2007) Arabidopsis isochorismate synthase functional in pathogen-induced salicylate biosynthesis exhibits properties consistent with a role in diverse stress responses. J Biol Chem **282:** 5919–5933

Tateda C, Zhang Z, Shrestha J, Jelenska J, Chinchilla D, Greenberg JT (2014) Salicylic acid regulates *Arabidopsis* microbial pattern receptor kinase levels and signaling. Plant Cell **26:** 4171–4187

Tatsuta T, Model K, Langer T (2005) Formation of membrane-bound ring complexes by prohibitins in mitochondria. Mol Biol Cell **16:** 248–259

Uknes S, Mauch-Mani B, Moyer M, Potter S, Williams S, Dincher S, Chandler D, Slusarenko A, Ward E, Ryals J (1992) Acquired resistance in *Arabidopsis*. Plant Cell **4:** 645–656

Van Aken O, Pecenková T, van de Cotte B, De Rycke R, Eeckhout D, Fromm H, De Jaeger G, Witters E, Beemster GTS, Inzé D, et al (2007) Mitochondrial type-I prohibitins of *Arabidopsis thaliana* are required for supporting proficient meristem development. Plant J **52:** 850–864

van Doorn WG, Beers EP, Dangl JL, Franklin-Tong VE, Gallois P, Hara-Nishimura I, Jones AM, Kawai-Yamada M, Lam E, Mundy J, et al (2011) Morphological classification of plant cell deaths. Cell Death Differ **18:** 1241–1246

van Verk MC, Bol JF, Linthorst HJ (2011) WRKY transcription factors involved in activation of SA biosynthesis genes. BMC Plant Biol **11:** 89

Verberne MC, Brouwer N, Delbianco F, Linthorst HJM, Bol JF, Verpoorte R (2002) Method for the extraction of the volatile compound salicylic acid from tobacco leaf material. Phytochem Anal **13:** 45–50

Vlot AC, Dempsey DA, Klessig DF (2009) Salicylic acid, a multifaceted hormone to combat disease. Annu Rev Phytopathol **47:** 177–206

Wang G, Zhang C, Battle S, Lu H (2014) The phosphate transporter PHT4; 1 is a salicylic acid regulator likely controlled by the circadian clock protein CCA1. Front Plant Sci **5:** 701

Wang H, Goffreda M, Leustek T (1993) Characteristics of an Hsp70 homolog localized in higher plant chloroplasts that is similar to DnaK, the Hsp70 of prokaryotes. Plant Physiol **102:** 843–850

Wang X, Gao J, Zhu Z, Dong X, Wang X, Ren G, Zhou X, Kuai B (2015) TCP transcription factors are critical for the coordinated regulation of isochorismate synthase 1 expression in *Arabidopsis thaliana*. Plant J **82:** 151–162

Wang Y, Ries A, Wu K, Yang A, Crawford NM (2010) The *Arabidopsis* Prohibitin gene *PHB3* functions in nitric oxide-mediated responses and in hydrogen peroxide-induced nitric oxide accumulation. Plant Cell **22:** 249–259

Wildermuth MC, Dewdney J, Wu G, Ausubel FM (2001) Isochorismate synthase is required to synthesize salicylic acid for plant defence. Nature **414:** 562–565

Yalpani N, Enyedi AJ, León J, Raskin I (1994) Ultraviolet light and ozone stimulate accumulation of salicylic acid, pathogenesis-related proteins and virus resistance in tobacco. Planta **193:** 372–376

Yamasaki K, Motomura Y, Yagi Y, Nomura H, Kikuchi S, Nakai M, Shiina T (2013) Chloroplast envelope localization of EDS5, an essential factor for salicylic acid biosynthesis in *Arabidopsis thaliana*. Plant Signal Behav **8:** e23603

Yao N, Greenberg JT (2006) *Arabidopsis* ACCELERATED CELL DEATH2 modulates programmed cell death. Plant Cell **18:** 397–411

Yuan Y, Chung JD, Fu X, Johnson VE, Ranjan P, Booth SL, Harding SA, Tsai CJ (2009) Alternative splicing and gene duplication differentially shaped the regulation of isochorismate synthase in Populus and Arabidopsis. Proc Natl Acad Sci USA **106:** 22020–22025

Zhang K, Halitschke R, Yin C, Liu CJ, Gan SS (2013) Salicylic acid 3-hydroxylase regulates Arabidopsis leaf longevity by mediating salicylic acid catabolism. Proc Natl Acad Sci USA **110:** 14807–14812

Zhang X, Henriques R, Lin SS, Niu QW, Chua NH (2006) Agrobacterium-mediated transformation of *Arabidopsis thaliana* using the floral dip method. Nat Protoc **1:** 641–646

Zhang Y, Xu S, Ding P, Wang D, Cheng YT, He J, Gao M, Xu F, Li Y, Zhu Z, et al (2010) Control of salicylic acid synthesis and systemic acquired resistance by two members of a plant-specific family of transcription factors. Proc Natl Acad Sci USA **107:** 18220–18225

Zhang Y, Zhao L, Zhao J, Li Y, Wang J, Guo R, Gan S, Liu CJ, Zhang K (2017) S5H/DMR6 encodes a salicylic acid 5-hydroxylase that fine-tunes salicylic acid homeostasis. Plant Physiol **175:** 1082–1093

Zhang Z, Shrestha J, Tateda C, Greenberg JT (2014) Salicylic acid signaling controls the maturation and localization of the Arabidopsis defense protein ACCELERATED CELL DEATH6. Mol Plant **7:** 1365–1383

Zheng XY, Spivey NW, Zeng W, Liu PP, Fu ZQ, Klessig DF, He SY, Dong X (2012) Coronatine promotes *Pseudomonas syringae* virulence in plants by activating a signaling cascade that inhibits salicylic acid accumulation. Cell Host Microbe **11:** 587–596

Zheng XY, Zhou M, Yoo H, Pruneda-Paz JL, Spivey NW, Kay SA, Dong X (2015) Spatial and temporal regulation of biosynthesis of the plant immune signal salicylic acid. Proc Natl Acad Sci USA **112:** 9166–9173